PCR with a sensitivity of 200 copies/ml to detect BKV. Quantitative PCR may be required to further clarify the impact of BKV infection on LHC.

The route of infection in patients with AdV-associated LHC has not been clarified. AdV can be transmitted by the inhalation of aerosolized virus and by the inoculation of virus into conjunctival sacs, but AdV-associated LHC was usually not preceded by symptoms of acute infection of the upper airway or conjunctiva. The fact that most adults have serum antibody to multiple serotypes of AdV also supports the notion that the reactivation of latent AdV infection, rather than acute infection, may be the major etiology of LHC. Interestingly, we identified male sex as a significant risk factor for the development of LHC. Similarly, the incidence of childhood HC is two to three times higher in boys than in girls.[8] Furthermore, AdV type 11 was shown to be the major causative agent in childhood HC, and its incidence is higher in Japan than in the West.[9] Considering all of these findings together, we considered the hypothesis that AdV type 11 may show tropism to a male-specific organ around the urinary tract, and acute infection in childhood may be followed by a latent infection in this organ. Reactivation of the virus in immunocompromised conditions after HSCT, especially in patients with acute GVHD, may cause LHC, and thus lead to a higher incidence in males.

Five of the six AdV-associated LHC patients examined had AdV type 11 viremia as proven by serum PCR. These serum samples were obtained during the episode of LHC. However, the clinical course of these patients was not different from that of the other LHC patients. On the other hand, some previous studies showed that the detection of AdV DNA in serum by PCR predicts the development of a severe or fatal AdV infection.[10,11] However, the previous study populations were different from ours; they included pediatric patients or recipients of T-cell-depleted hematopoietic stem cell transplantation. Furthermore, most of these studies did not analyze AdV type 11 but type 1, 2, 5, 12, 31, 34, and 35 infections. Therefore, we considered that the impact of AdV viremia may differ among patient populations, the level of immunosuppression, and/or the serotype of AdV.

In conclusion, LHC after HSCT was predominant in males and patients who developed acute GVHD. The detection of AdV type 11 DNA by serum PCR was not associated with severe AdV infection in this population. However, these findings should be validated in other Japanese adult populations.

References

1 Sencer SF, Haake RJ, Weisdorf DJ. Hemorrhagic cystitis after bone marrow transplantation. Risk factors and complications. *Transplantation* 1993; **56**: 875–879.
2 Miyamura K, Takeyama K, Kojima S *et al.* Hemorrhagic cystitis associated with urinary excretion of adenovirus type 11 following allogeneic bone marrow transplantation. *Bone Marrow Transplant* 1989; **4**: 533–535.
3 Akiyama H, Kurosu T, Sakashita C *et al.* Adenovirus is a key pathogen in hemorrhagic cystitis associated with bone marrow transplantation. *Clin Infect Dis* 2001; **32**: 1325–1330.
4 Azzi A, Fanci R, Bosi A *et al.* Monitoring of polyomavirus BK viruria in bone marrow transplantation patients by DNA hybridization assay and by polymerase chain reaction: an approach to assess the relationship between BK viruria and hemorrhagic cystitis. *Bone Marrow Transplant* 1994; **14**: 235–240.
5 Seber A, Shu XO, Defor T *et al.* Risk factors for severe hemorrhagic cystitis following BMT. *Bone Marrow Transplant* 1999; **23**: 35–40.
6 Leung AY, Mak R, Lie AK *et al.* Clinicopathological features and risk factors of clinically overt haemorrhagic cystitis complicating bone marrow transplantation. *Bone Marrow Transplant* 2002; **29**: 509–513.
7 Robert JG. A class of K-sample test for comparing the cumulative incidence of a competing risk. *Ann Stat* 1988; **16**: 1141–1154.
8 Kondo M, Kojima S, Kato K, Matsuyama T. Late-onset hemorrhagic cystitis after hematopoietic stem cell transplantation in children. *Bone Marrow Transplant* 1998; **22**: 995–998.
9 Mufson MA, Belshe RB. A review of adenoviruses in the etiology of acute hemorrhagic cystitis. *J Urol* 1976; **115**: 191–194.
10 Chakrabarti S, Mautner V, Osman H *et al.* Adenovirus infections following allogeneic stem cell transplantation: incidence and outcome in relation to graft manipulation, immunosuppression, and immune recovery. *Blood* 2002; **100**: 1619–1627.
11 Echavarria M, Forman M, van Tol MJ *et al.* Prediction of severe disseminated adenovirus infection by serum PCR. *Lancet* 2001; **358**: 384–385.

THE JOURNAL OF BIOLOGICAL CHEMISTRY
Vol. 279, No. 15, Issue of April 9, pp. 15630–15638, 2004
Printed in U.S.A.

AML1 Is Functionally Regulated through p300-mediated Acetylation on Specific Lysine Residues*

Received for publication, January 13, 2004
Published, JBC Papers in Press, January 29, 2004, DOI 10.1074/jbc.M400355200

Yuko Yamaguchi‡, Mineo Kurokawa‡‖, Yoichi Imai‡, Koji Izutsu‡, Takashi Asai‡, Motoshi Ichikawa‡, Go Yamamoto‡, Eriko Nitta‡, Tetsuya Yamagata‡, Kazuki Sasaki§, Kinuko Mitani¶, Seishi Ogawa‡, Shigeru Chiba‡, and Hisamaru Hirai†‡

From the ‡Department of Hematology and Oncology, Graduate School of Medicine, University of Tokyo, Tokyo 113-8655, the §Growth Factor Division, National Cancer Center Research Institute, Tokyo 104-0045, and the ¶Department of Hematology, Dokkyo University School of Medicine, Mibu, Tochigi 321-0293, Japan

***AML1* (*RUNX1*) is one of the most frequently disrupted genes in human leukemias. *AML1* encodes transcription factors, which play a pivotal role in hematopoietic differentiation, and their inappropriate expression is associated with leukemic transformation of hematopoietic cells. Previous studies demonstrated that the transcription cofactor p300 binds to the C-terminal region of AML1 and stimulates AML1-dependent transcription during myeloid cell differentiation. Here, we report that AML1 is specifically acetylated by p300 *in vitro*. Mutagenesis analyses reveal that p300 acetylates AML1 at the two conserved lysine residues (Lys-24 and Lys-43). AML1 is subject to acetylation at the same sites *in vivo*, and p300-mediated acetylation significantly augments the DNA binding activity of AML1. Disruption of these two lysines severely impairs DNA binding of AML1 and reduced the transcriptional activity and the transforming potential of AML1. Taken together, these data indicate that acetylation of AML1 through p300 is a critical manner of posttranslational modification and identify a novel mechanism for regulating the function of AML1.**

AML1 (PEBP2αB, core binding factor α2, or RUNX1) and its cofactor PEBP2β/core binding factor β are the most frequent targets of chromosomal translocations in human leukemias (1). The *AML1* gene was identified through its involvement in the (8;21) translocation, which rearranges the *AML1* gene on chromosome 21q22 and the *ETO* (*MTG8*) gene on chromosome 8q22, resulting in the generation of the AML1-ETO fusion protein (2–4). *AML1* is also involved in human leukemias carrying t(3;21) or t(12;21) translocation, suggesting that it plays an important role in leukemogenesis (5–8).

The *AML1* gene encodes a transcription factor containing an N-terminal DNA-binding domain that is highly homologous to the *Drosophila* pair-rule protein Runt, which is called the Runt domain (9). AML1 binds to the core enhancer DNA sequence, TG(T/c)GGT, called the PEBP2 site, through the Runt domain. Its affinity for DNA is markedly increased by heterodimerization with PEBP2β (10–13). This heterodimeric complex regulates transcription of a large number of hematopoietic lineage-specific genes (14, 15). Targeted disruption of either *AML1* or *PEBP2β* has demonstrated that both AML1 and PEBP2β are essential for all lineages of definitive hematopoiesis in the murine fetal liver (16–18). In addition, AML1 exhibits the transforming activity when expressed in fibroblasts, and this activity requires both the Runt domain and the C-terminal transcriptional regulatory domain called the PST region (19). At least four forms of the AML1 proteins are produced by alternative splicing, termed AML1a, AML1b, AML1c, and AML1ΔN (20, 21). Among them, AML1b is one of the transcriptionally active forms, which contain both the Runt domain and the PST region (22). We simply refer to this alternative form as AML1 hereafter.

Previously, Kitabayashi *et al.* (23) demonstrated that AML1 associates with a transcription cofactor p300 *in vivo* and that p300 potentiates AML1-dependent transcriptional activation. On the other hand, AML1 synergizes with a variety of transcription factors, including CCAAT/enhancer binding protein-α, AP-1, Ets-1, PU.1, and c-Myb, which regulate cellular proliferation and differentiation (24–30). Conversely, AML1 can repress transcription by associating with corepressors such as Groucho/transducin-like Enhancer of split and mSin3A (31–33). Thus, AML1 appears to act as an "organizing" factor of transcription by interacting with a wide variety of transcription regulators. In contrast, regulatory mechanisms for AML1 function remain elusive thus far. Previously, we reported that AML1 is phosphorylated through the extracellular signal-regulated kinase (ERK)[1] (34). ERK-dependent phosphorylation potentiates the transactivation ability and the transforming capacity of AML1 through regulating interaction between AML1 and mSin3A (35). Thus, the function of AML1 is also regulated through the signal transduction pathways.

Acetylation has recently emerged as the central mode of regulation for a significant number of transcription factors (36, 37). p300 and the related protein CBP are highly conserved proteins that have a pivotal role in transcriptional regulation, bridging a wide variety of DNA-binding proteins to components of the general transcriptional machinery (38). In addition, p300

* This work was partially supported by a fellowship from the Ministry of Education, Culture, Sports, Science and Technology of Japan. The costs of publication of this article were defrayed in part by the payment of page charges. This article must therefore be hereby marked "*advertisement*" in accordance with 18 U.S.C. Section 1734 solely to indicate this fact.

†Hisamaru Hirai died suddenly on August 23, 2003. His students, fellows, and colleagues will greatly miss his energetic and nurturing leadership in the field of hematology. We dedicate this paper in his memory.

‖ To whom correspondence should be addressed: Dept. of Hematology and Oncology, Graduate School of Medicine, University of Tokyo, 7-3-1 Hongo, Bunkyo-ku, Tokyo 113-8655, Japan. Tel.: 81-3-5800-6528; Fax: 81-3-3815-8350; E-mail: kurokawa-tky@umin.ac.jp.

[1] The abbreviations used are: ERK, extracellular signal-regulated kinase; HAT, histone acetyltransferase; GST, glutathione *S*-transferase; EMSA, electrophoretic mobility shift assay; CBP, CREB-binding protein; CREB, cAMP-response element-binding protein; luc, luciferase; PST region, a proline-, serine-, and threonine-rich region; P/CAF, p300/CBP-associated factor; M-CSF receptor, macrophage colony-stimulating factor receptor.

and CBP possess histone acetyltransferase (HAT) activity, which is able to acetylate histone and non-histone proteins. Histone acetylation is linked to transcriptional activation and participates in the nucleosomal remodeling that accompanies gene activity (39). Recently, HATs have been shown to also acetylate a significant number of non-histone proteins, which include transcription factors such as p53, *Drosophila* T-cell receptor, erythroid kruppel-like factor, GATA-1, GATA-3, and the high mobility group protein I/Y (40, 41). Acetylation of these factors leads to changes in protein-protein and protein-DNA interaction, which subsequently result in altered gene expression (42). Here we report that AML1 is acetylated by p300 at the two lysine residues located in the N terminus adjacent to the Runt domain. Acetylation of AML1 significantly increases the amount of AML1 bound to DNA and results in stimulation of AML1-dependent transcription. Substitution of target residues uncovered a close relationship between the acetylation and the *in vivo* function of AML1. Our studies demonstrate that acetylation is a critical manner of posttranslational modification of AML1.

MATERIALS AND METHODS

Cell Cultures—COS7, 293T, HeLa, and NIH3T3 cells were maintained in Dulbecco's modified Eagle's medium supplemented with penicillin, streptomycin, and 10% fetal calf serum at 37 °C in a 5% CO_2 incubator. M1 cells and MOLT-4 cells were cultured in Dulbecco's modified Eagle's medium and α-minimal essential medium by one to one and RPMI 1640 medium, respectively, which contain penicillin, streptomycin, and 10% fetal calf serum.

Plasmid Constructions and Recombinant Proteins—pGEX-AML1-(1–189), pGEX-K24R/K43R-(1–189), and pGEX-K24A/K43A-(1–189) were obtained by cloning the PCR fragments corresponding to amino acids 1–189 of AML1, K24R/K43R, and K24A/K43A into the pGEX2T vector, respectively. For construction of FLAG-tagged P/CAF-HAT/Br and GCN5, the DNA fragments corresponding to amino acids 352–832 and amino acids 1–477, respectively, were amplified by PCR and subcloned into pFLAG-MAC (Kodak). The expression plasmids for GST-PEBP2β and FLAG-tagged p300-HAT were constructed as described previously (43, 44). Construction of pME18S-AML1 and AML1Δ-(47–172) was described elsewhere (19, 45). For construction of Δ-(23–64), a fragment for amino acids 1–64 of AML1 was replaced by a fragment for amino acids 1–22 generated by a PCR method. For construction of Δ-(173–188), the ApaI-SalI fragment of AML1 was replaced by the corresponding fragment that lacks the region between amino acids 173 and 188, which was generated by a PCR method. For tagging AML1 and deletion mutants at the N terminus, the FLAG octapeptide (DYKDDDDK) was inserted after the first methionine by PCR as described previously (32). The AML1 K24R, K43R, K24R/K43R, K24A/K43A, K182R, K188R, and K182R/K188R were obtained by replacing the lysine residues with arginines and alanines, respectively, by the site-directed mutagenesis method (46). For construction of the retroviral vector that harbors AML1 or K24A/K43A, the 1.8-kb EcoRI fragment encoding AML1 or K24A/K43A was deprived of the polyadenylation signal by digestion with BamHI and cloned into the pSRαMSVtk*neo* vector (19). pM-CSF-R-luc containing −416 to +71 of the human M-CSF receptor promoter was described previously (47). pcDEF3-p300 was kindly provided by Dr. Miyazono and Dr. Kawabata. The glutathione *S*-transferase (GST) fusion constructs of AML1, FLAG-tagged p300-HAT, P/CAF-HAT/Br, and GCN5 were purified as described previously (44, 45).

In Vitro Acetylation Assays—GST fusion proteins or histones (Roche Applied Science) were collected on glutathione-Sephahrose beads (Amersham Biosciences), incubated at 30 °C for 1 h in the buffer containing 50 mM Tris, pH 8.0, 10% glycerol, 1 mM dithiothreitol, 1 mM phenylmethylsulfonyl fluoride, 10 mM sodium butyrate, and 0.05 μCi of [^{14}C]acetyl-CoA (Amersham Biosciences), and analyzed by sodium dodecyl sulfate-polyacrylamide gel electrophoresis (SDS-PAGE).

Transfection, Immunoprecipitation, and Immunoblot Analysis—COS7 cells or 293T cells were transfected with expression plasmids by the DEAE-dextran method as described previously (48). Polyclonal antisera to the full-length (anti-AML1), the PST region (anti-PST) of AML1, and PEBP2β (anti-PEBP2β) were raised in rabbit against bacterially produced proteins as described previously (43, 45, 49). For detection of p300 and AML1 proteins, the indicated cells were lysed in the buffer containing 350 mM NaCl, 50 mM Tris-HCl (pH 7.5), 0.5% Igepal, 1 mM EDTA, 0.5 mM dithiothreitol, 10 mM sodium butyrate, 1 μg of aprotinin/ml, 1 μg of pepstatin/ml, 1 μg of leupeptin/ml, 0.2 mM phenylmethylsulfonyl fluoride followed by incubation for 30 min on ice. Whole cell lysates containing 100 μg of proteins were subjected to SDS-PAGE and transferred to polyvinylidene difluoride membranes (Immobilon, Millipore). The membranes were blocked with 10% skim milk, treated with anti-p300 (RW128, Upstate Biotechnology), anti-AML1, anti-FLAG (M2; Sigma), or anti-PEBP2β, washed, and reacted with the mouse or rabbit anti-IgG antibody coupled to horseradish peroxidase. The blots were visualized using the enhanced chemiluminescence (ECL) system (Amersham Biosciences). For immunoprecipitation, cells were lysed in the above buffer and subjected to immunoprecipitation with anti-PST or anti-AML1 (PC284L; Oncogene) followed by absorption to protein A-Sepharose (Sigma). Immunoprecipitates were washed, separated by SDS-PAGE, and analyzed with anti-p300 as described above.

In Vivo Sodium [^{3}H]Acetate Labeling—MOLT-4 cells were grown to 2×10^7 cells, washed twice with cold phosphate-buffered saline, resuspended in RPMI labeling medium (1 mCi of ^{3}H-sodium acetate (Amersham Biosciences) per ml and 50 nM trichostatin A (Wako)), and then incubated at 37 °C for 90 min. pME18S-AML1 and mutants either with or without FLAG tag were transfected with pcDEF3-p300 as described above into COS7 cells. After 30 h, cells were exposed to 1 mCi of sodium [^{3}H]acetate/ml in the presence of 50 nM trichostatin A for 90 min. Lysates were prepared and processed using either anti-PST or anti-FLAG as described above and resolved by SDS-PAGE. Proteins were electrotransferred onto polyvinylidene difluoride membrane (Immobilon, Millipore) and analyzed using BAS2000 Image Analyzer (Fuji Film).

Electrophoretic Mobility Shift Assay (EMSA)—The M4 probe containing a partial A core of the polyomavirus enhancer was produced as described elsewhere (50). Five micrograms of GST fusion proteins were collected on glutathione-Sepharose beads, incubated with purified FLAG-p300-HAT in the presence or absence of 10 nM acetyl-CoA (Amersham Biosciences). Then, reaction mixtures were eluted from the beads in glutathione elution buffer (10 mM reduced glutathione in 50 mM Tris-HCl (pH 8.0)). GST-PEBP2β collected on glutathione-Sepharose beads was incubated in the thrombin (Amersham Biosciences) reaction mixture at room temperature for 16 h, and then centrifuged, and supernatant containing PEBP2β cleaved off from GST was collected. The recovered proteins were quantified by Coomassie staining, and 100 ng of these proteins were incubated with 1 ng of M4 probe in the buffer containing 20 mM Hepes (pH 7.6), 4% Ficoll (W/V), 10 mM EDTA, 40 mM KCl, 0.5 mM dithiothreitol, 300 ng of poly(dI-dC) for 30 min at room temperature in the presence or absence of PEBP2β. Seventy ng of unlabeled M4 probe were added as a cold competitor. Reaction mixtures were subjected to EMSA as described previously (45). Nuclear extracts were obtained from COS7 cells transfected with full-length AML1 or K24R/K43R in pME18S either alone or together with PEBP2β by the DEAE-dextran method, as described previously (19). The procedures for EMSA were presented previously (45). For radioisotope labeling, [α-^{32}P]dCTP was incorporated into the M4 probe by incubating with the Klenow fragment.

Luciferase Assays—HeLa cells were transfected by using SuperFect (Qiagen) with pM-CSF-R-luc and plasmids expressing wild type AML1, K24R/K43R, or K24A/K43A in the presence or absence of p300 expression plasmids. Fifty ng/ml trichostatin A was added 8 h prior to harvest. Luciferase activity was determined 48 h later, as described previously (51). A plasmid expressing β-galactosidase was co-transfected as an internal control of transfection efficiency, and the data were normalized to the β-galactosidase activity, as described previously (51).

Soft Agar Assays—Soft agar assays were performed according to procedures described elsewhere (19, 52). Colonies were counted after 14 days of culture in soft agar if they were larger than 0.25 mm in diameter.

RESULTS

AML1 Interacts with p300 in Vivo—p300 and CBP are known to interact with a variety of transcriptional factors as coactivators. Recently, a physical interaction between AML1 and p300 was demonstrated (23). To confirm the interaction of endogenous AML1 with p300 in hematopoietic cells, we performed immunoprecipitation experiments using M1 cells, a murine leukemic cell line. Whole cell lysates were prepared from M1 cells and subjected to immunoprecipitation with the anti-AML1 antibody or control preimmune serum. Immunoblot

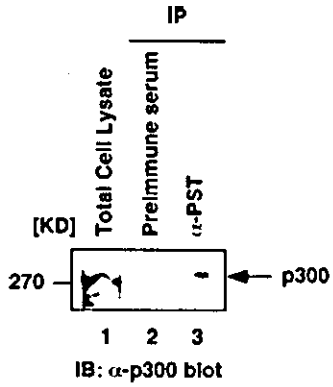

FIG. 1. **AML1 interacts with p300 *in vivo*.** Co-immunoprecipitation (*IP*) of endogenous AML1 with p300 in lysates from M1 cells is shown. Whole cell lysates were precipitated with preimmune serum (*lane 2*) or anti-PST serum (*lane 3*), and the precipitate was subjected to immunoblot (*IB*) analysis with anti-p300.

analysis with the p300-specific antibody showed that the precipitate with anti-AML1 contained p300, whereas p300 protein was never detected in the precipitate obtained with control preimmune serum (Fig. 1). These results indicate that AML1 forms complexes with p300 *in vivo* in agreement with previous findings (23).

p300 Specifically Acetylates AML1 in Vitro—Association of p300 with AML1, together with the recent demonstration of its acetyltransferase activity on a variety of transcription factors, prompted us to determine whether AML1 is a substrate for acetylation by p300. AML1 possesses nine lysine residues, which become potential targets for acetylation. To examine whether AML1 could be acetylated by p300 directly, the *in vitro* acetylation assays were performed using bacterially expressed FLAG-tagged HAT domain of p300 (p300-HAT). GST was fused to a region between amino acids 1 and 189 of AML1 (AML1-(1–189)), which contains all nine lysine residues, and the GST fusion protein was expressed in the BL21 bacterial host and purified (Fig. 2*A*). GST-AML1-(1–189) was incubated with p300-HAT in the presence of [^{14}C]acetyl-CoA. Use of these highly purified recombinant proteins eliminates possible contamination by other HATs. As shown in Fig. 2*B*, GST-AML1-(1–189) was specifically labeled with [^{14}C]acetyl-CoA in the presence of p300-HAT, whereas no signal was detected for GST alone. The faster migrating bands were considered to represent degraded products of the acetylated AML1 protein because the purified GST-AML1-(1–189) that served as a substrate contains identically migrating bands. In contrast, GST-AML1-(1–189) was never labeled without p300-HAT. We further investigated whether other HATs can acetylate AML1 using P/CAF and its close homologue GCN5. The HAT/bromodomain of P/CAF (P/CAF-HAT/Br) and full-length GCN5 were tagged with FLAG, expressed bacterially, and subsequently used in the *in vitro* acetylation assays. The results in Fig. 2*B* show that neither P/CAF-HAT/Br nor GCN5 acetylated GST-AML1-(1–189) at all. As shown in Fig. 2*C*, the HAT activities of p300-HAT, P/CAF-HAT/Br, and GCN5 were confirmed by using histones as substrates. p300-HAT could acetylate histones H2A, H2B, H3, and H4, whereas only histones H3 and H4 were acetylated by P/CAF-HAT/Br and GCN5, which is in agreement with the previous reports (42). Taken together, these results unequivocally indicate that AML1 can be a specific substrate for p300-mediated acetylation *in vitro*.

In Vivo Acetylation of AML1—Next, we went on further to examine whether acetylation of AML1 occurs *in vivo* to manifest a physiological relevance of *in vitro* acetylation of AML1. First, we wished to determine whether endogenous AML1 in hematopoietic cells was also acetylated. For these experiments, we pulse-labeled MOLT-4 cells, a human acute lymphoblastic leukemia cell line, with [^{3}H]acetate in the presence of a histone deacetylase inhibitor (trichostatin A) and then subjected them to cell lysis and immunoprecipitation with anti-AML1. As shown in Fig. 3*A*, anti-AML1, but not control preimmune serum, precipitated [^{3}H]acetate-labeled AML1 (*lanes 2* and *3*). Immunoblot analysis with the same antibody revealed migration of endogenous AML1 (*lane 1*). These results directly provide evidence that AML1 is endogenously acetylated in hematopoietic cells.

To define the positions within AML1 to be acetylated by p300, we then employed transient transfection into COS7 cells. First, cells were transfected with FLAG-tagged full-length AML1 and p300 and labeled with sodium [^{3}H]acetate in the same manner performed above. Lysates were immunoprecipitated with the anti-FLAG antibody and subjected to immunoblot analysis. As shown in Fig. 3*B*, AML1 was efficiently recovered from AML1-transfected cells with anti-FLAG. The immunoprecipitated AML1 protein was specifically labeled with [^{3}H]acetate as in MOLT-4 cells (Fig. 3*B*, *right*). Next, we employed three types of serial deletion mutants to cover all nine lysines (Fig. 2*A*). These FLAG-tagged mutants were expressed in COS7 cells together with p300 and subjected to the *in vivo* acetylation assays. Fig. 3*B* shows that these mutants are expressed in COS7 cells in the anticipated sizes. Acetylation of AML1 was retained when amino acids 47–172 in the Runt domain or amino acids 173–188 in C-terminal region adjacent to the Runt domain are deleted (*lanes 9* and *10*). In contrast, deletion of N-terminal region (amino acids 23–64) flanked by the Runt domain completely abolished AML1 acetylation by p300 (*lane 8*). This region contains two lysine residues, Lys-24 and Lys-43. These two lysines are highly conserved among the Runt-containing protein family, with Lys-24 being completely conserved from the Zebrafish Runx1 to the human AML1 family members. These results suggest that either or both of these two N-terminal lysines are potentially acetylated by p300.

AML1 Is Acetylated by p300 on N-terminal Two Lysine Residues—To precisely determine the target residues of AML1 for p300-mediated acetylation, Lys-24 and Lys-43 were substituted with arginines or alanines either individually or in combination. Substitution of either Lys-24 or Lys-43 with arginine (K24R or K43R) significantly reduced the level of acetylation. The level of acetylation in K24R was significantly lower than that in K43R. Furthermore, substitution of both Lys-24 and Lys-43 by arginines or alanines almost completely abolished acetylation of AML1 (Fig. 4*B*). In contrast, substitution of C-terminal lysines (Lys-182 and Lys-188) did not alter *in vivo* acetylation of AML1, indicating that these residues are not involved in acetylation. These findings suggest that Lys-24 and Lys-43 are preferentially acetylated *in vivo* in agreement with the results obtained from the deletion mutants. We also performed an *in vitro* acetylation assay using purified forms of GST-K24R/K43R-(1–189) and GST-K24A/K43A-(1–189) in which Lys-24 and Lys-43 of AML1-(1–189) were substituted by arginines and alanines, respectively. Although GST-AML1-(1–189) was efficiently acetylated by p300, no acetylation was detected for GST-K24R/K43R-(1–189) and GST-K24A/K43A-(1–189) (Fig. 4*C*), which is consistent with the results of the *in vivo* acetylation assays. Autoacetylated p300-HAT was observed in the very top in all lanes except the one without p300-HAT. To preclude the possibility that substitution of Lys-24 and Lys-43 can disrupt the interaction between AML1 and p300, we performed immunoprecipitation experiments by transiently expressing p300 with AML1 and K24A/K43A in 293T cells. The mutant formed a complex with p300 as effi-

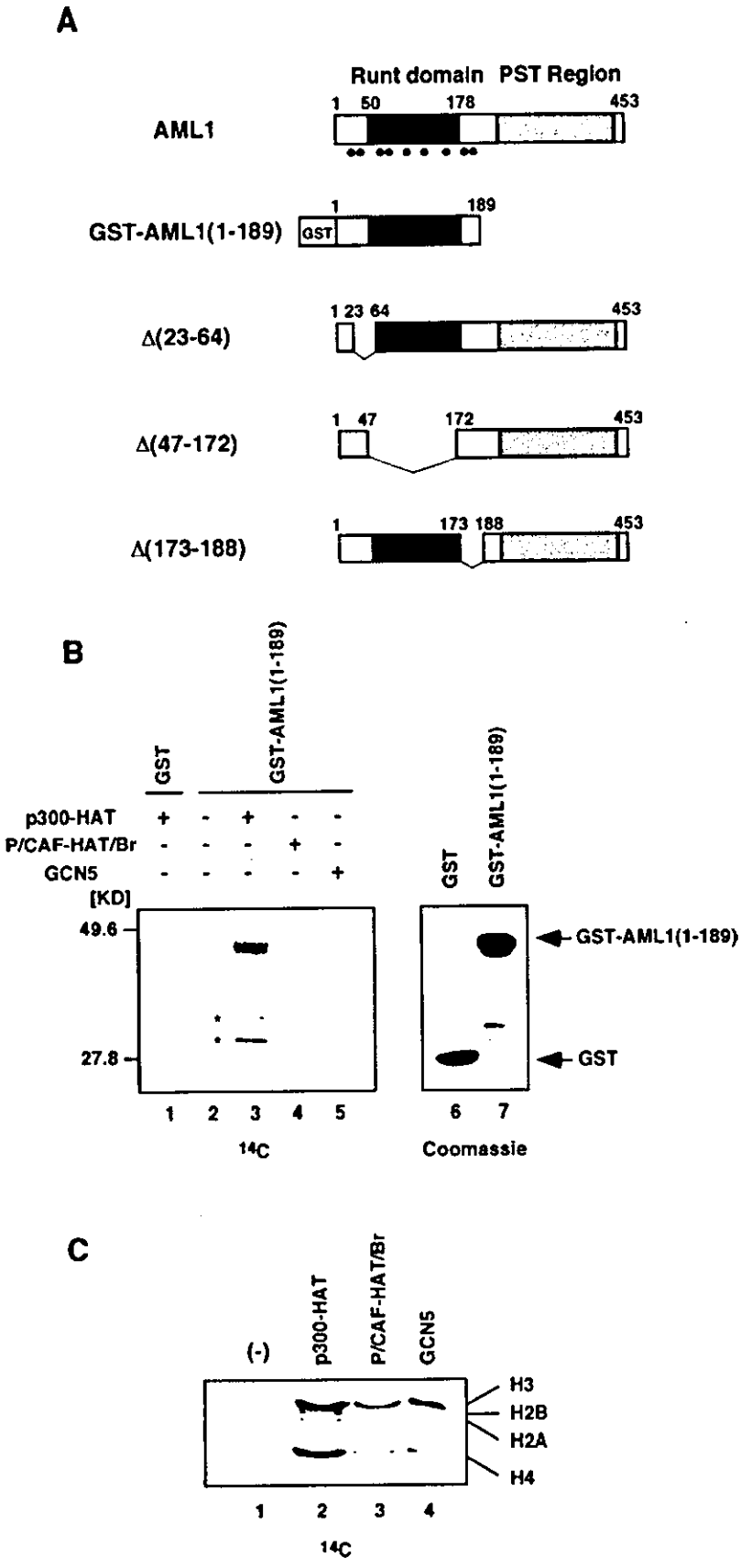

FIG. 2. ***In vitro* acetylation of AML1 by p300-HAT.** *A*, structures of AML1 and GST-AML1 fusion constructs used as substrates for p300. The Runt domain is *closed*. The PST region and GST are *shaded*. The positions of lysine residues are indicated by the *closed circles*. *B*, the *in vitro* acetylation assay of AML1 with p300-HAT, P/CAF-HAT/Br, and GCN5. Purified GST or GST-AML1-(1–189) protein was incubated with or without each recombinant HAT in the presence of [^{14}C]acetyl-CoA for 1 h at 30 °C. Reaction products were resolved by SDS-PAGE (*lanes 1–5*). The gel was stained with Coomassie Blue to demonstrate that the equivalent substrate was used in each reaction (*lanes 6* and *7*). *Asterisks* indicate degraded products of acetylated AML1. *C*, histone acetylation by various HATs. Histones (H2A, H2B, H3, and H4) were incubated either with or without each recombinant HAT in the presence of [^{14}C]acetyl-CoA for 1 h at 30 °C followed SDS-PAGE as described above.

ciently as wild type AML1 in 293T cells (data not shown). These results imply that loss of acetylation in the Lys-24/Lys-43 mutant does not result from their inability to associate with p300 but suggest that these two lysines are authentic targets for acetylation by p300.

Acetylation Augments Site-specific DNA Binding of AML1—Having identified an AML1 mutant that cannot be acetylated by p300, we set out to use this mutant to dissect the functional consequence of AML1 acetylation. For a growing number of transcription factors, it has been suggested that acetylation

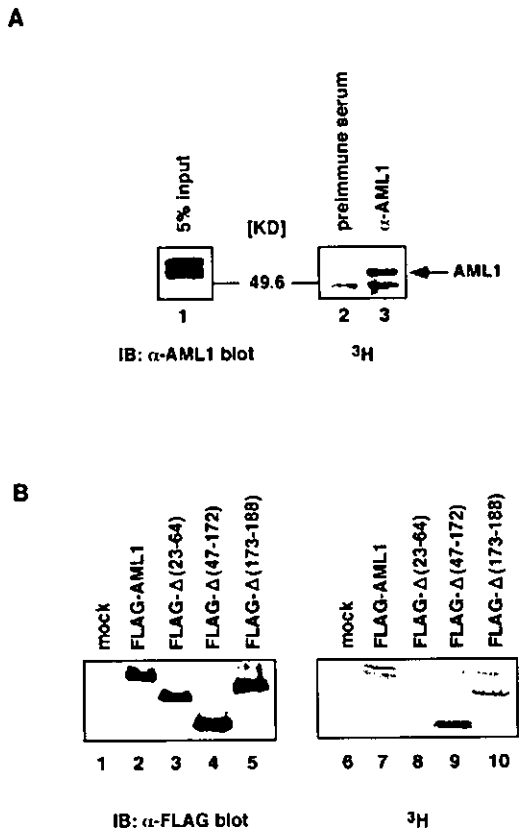

FIG. 3. **Acetylation of AML1 *in vivo*.** *A*, lysates from MOLT-4 cells pulse-labeled with 1 mCi of sodium ^{3}H/ml in the presence of 50 nM trichostatin A were immunoprecipitated with anti-AML1 or preimmune serum as a control. Immunoprecipitated samples were resolved by SDS-PAGE. Proteins were electrotransferred onto polyvinylidene difluoride membrane and immunoblotted (*IB*) with anti-AML1 (*lane 1*) or analyzed using BAS2000 image analyzer (*lanes 2* and *3*). Input represents 5% of the radiolabeled protein used in the assay. Locations of molecular mass markers and AML1 are shown. *B*, COS7 cells were transfected with 10 μg of pME18S, FLAG-tagged wild type AML1, or the FLAG-tagged deletion mutants of AML1, together with pcDEF3-p300 as indicated, and were labeled with sodium [^{3}H]acetate in the presence of trichostatin A. Whole cell lysates were immunoprecipitated with anti-PST and subsequently resolved on SDS-PAGE (*right*). Expression of each protein is monitored by immunoblotting of whole cell lysates with anti-FLAG (*left*). *mock*, mock-infected.

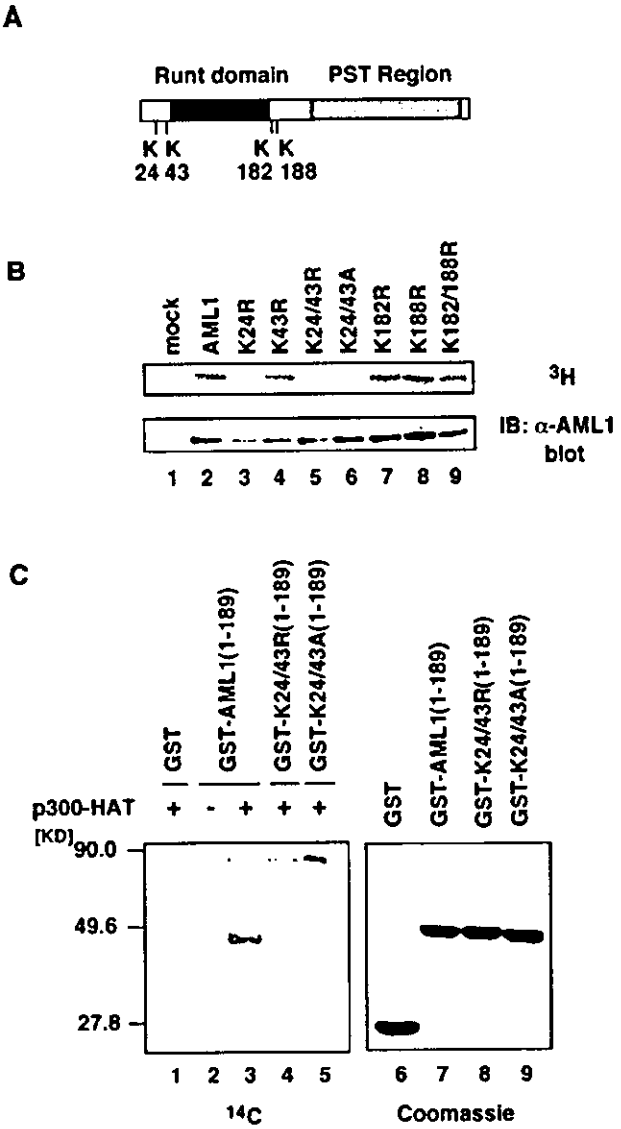

FIG. 4. **Determination of lysine residues acetylated by p300.** *A*, positions of lysine residues outside the Runt domain. *B*, the lysine mutants of AML1 were transfected into COS7 cells together with pcDEF3-p300. Transfected cells were pulse-labeled with sodium [^{3}H]acetate for 90 min. Whole cell lysates were immunoprecipitated with anti-PST and resolved by SDS-PAGE (*top*). The expression levels of each construct were monitored by immunoblotting (*IB*) of whole cell lysates with anti-AML1 (*bottom*). *mock*, mock-infected. *C*, GST fusion proteins were incubated with or without purified FLAG-tagged p300-HAT in the presence of [^{14}C]acetyl-CoA, as indicated. Reaction mixtures were separated by SDS-PAGE, fixed, and stained with Coomassie Blue (*lanes 6–9*). The stained gel was dried, and ^{14}C incorporation was visualized by BAS2000 image analyzer (*lanes 1–5*).

plays a key role in the regulation of sequence-specific DNA binding (40, 42). Since acetylation can lead to a change in the charge and the size of the lysine residues (53), it is likely that acetylation impinges on the affinity of AML1 for DNA. To test this possibility, electrophoretic mobility shift assays were performed with purified proteins for GST-AML1-(1–189) or its lysine mutant, both of which possess the Runt domain that is responsible for binding to the PEBP2 site (11, 12). Each protein was incubated with bacterially produced p300-HAT and radiolabeled M4 probe, double-stranded oligonucleotide bearing the PEBP2 site, and DNA binding abilities were evaluated. When M4 probe was incubated with GST-AML1-(1–189) and p300-HAT in the absence of acetyl-CoA, we observed a shifted band that was not seen for GST (Fig. 5*A*, *left*). The shifted band was significantly reduced when an excess of the cold probe was added, indicating that the AML1-DNA complex was formed through specific binding of AML1 to the PEBP2 sequence. We then determined the effect of p300-mediated acetylation on DNA binding of AML1. The addition of acetyl-CoA greatly augmented the shifted band (Fig. 5*A*, *left*, *lane 4*), indicating DNA binding of AML1 specifically enhanced by acetylation. In contrast, K24R/K43R substitution in GST-AML1-(1–189) significantly abolished the DNA binding ability of AML1, and no increase in DNA binding was found even upon the treatment of acetyl-CoA (Fig. 5*A*, *left*, *lanes 5* and *6*). Coomassie staining of each recombinant protein indicated the presence of equal amounts of the GST-AML1 proteins (Fig. 5*A*, *right*).

Because PEBP2β is a key regulator for DNA binding of AML1, we next tested the effect of AML1 acetylation on DNA binding in the presence of PEBP2β. As shown in Fig. 5*B* (*left*), GST-AML1-(1–189) in the presence of bacterially produced PEBP2β showed a sequence-specific DNA-binding complex that was markedly diminished by the addition of the cold probe. K24A/K43A mutation abolished the DNA binding ability of AML1 even in the presence of PEBP2β (Fig. 5*B*, *left*). The K24R/K43R mutant, which maintains the positive charge also exhibited severely impaired DNA binding, indicating that al-

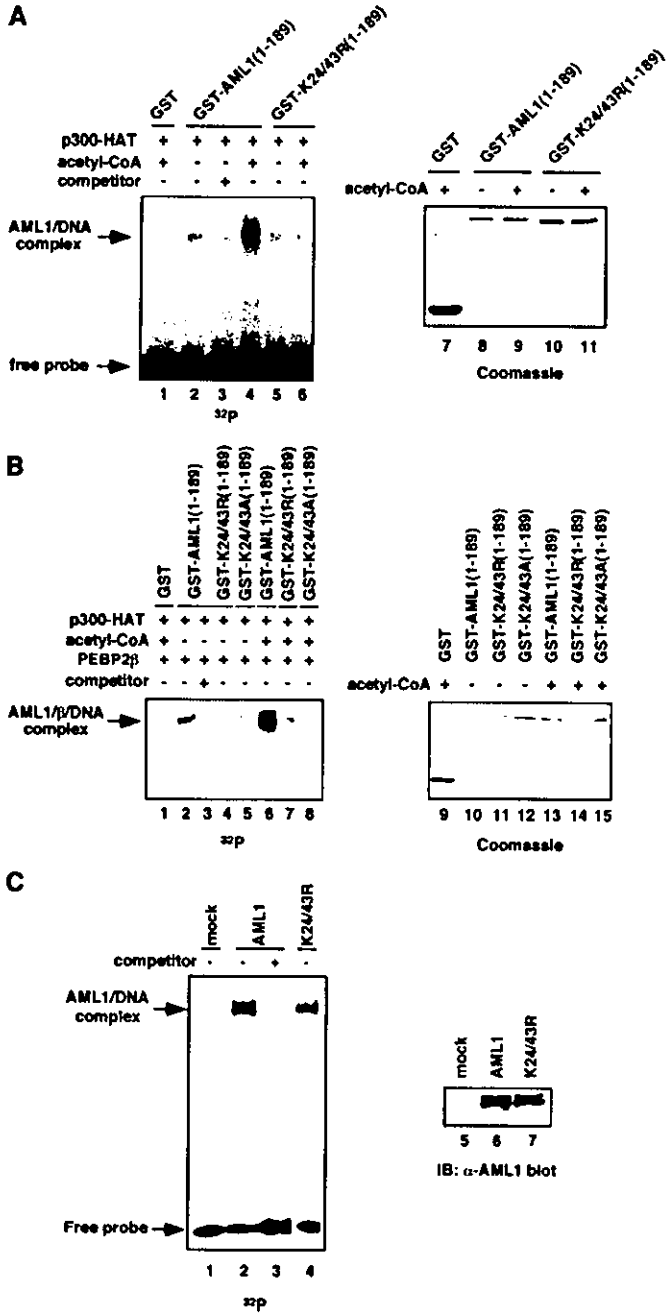

FIG. 5. **The DNA binding activity of AML1 is augmented by acetylation.** *A*, EMSAs demonstrating DNA binding of acetylated and unmodified AML1. Purified GST, GST-AML1-(1–189), or its lysine mutant (GST-K24R/K43R-(1–189)) was incubated with p300-HAT and the ^{32}P-labeled M4 probe either in the presence or in the absence of acetyl-CoA, as indicated (*left*). Excess of the unlabeled M4 probe was used as a competitor. Amounts of purified GST fusion proteins used in EMSA were monitored by Coomassie staining (*right*). *B*, DNA binding of unmodified (*lanes 2–5*) and *in vitro* acetylated GST, GST-AML1-(1–189), or its lysine mutant (GST-K24R/K43R or A-(1–189)) (*lanes 6–8*) was tested by EMSA as indicated above in the presence of bacterially expressed and purified PEBP2β (*left*). Coomassie staining exhibits the equal amounts of GST fusion proteins used in EMSA (*right*). *C*, the ^{32}P-labeled M4 probe was co-incubated with nuclear extracts (containing 18 μg of proteins) from COS7 cells co-transfected with the control vector, the wild type of full-length AML, or K24R/K43R together with PEBP2β (*left*). Expression of each protein was monitored (*right*). *IB*, immunoblot.

tered DNA binding results from a block of acetylation of Lys-24/Lys-43 rather than a fundamental change in the conformation of the mutants. Impaired DNA binding in these mutants was not restored by the addition of acetyl-CoA, which significantly enhanced DNA binding of the AML1-PEBP2β complex. Coomassie staining of each recombinant protein indicated the presence of equal amounts of the GST-AML1 proteins (Fig. 5*B*, *right*). These results indicate that PEBP2β cannot fully overcome a decrease in DNA binding of the AML1 mutants defective for acetylation.

To obtain further evidence that acetylation of target lysines alters DNA binding of AML1, we examined the effect of acetylation on sequence-specific DNA binding using full-length AML1 and its arginine mutant (K24R/K43R) in the presence of PEBP2β. We performed EMSA with nuclear extracts of COS7 cells transfected with mock, full-length AML1, and K24R/K43R together with PEBP2β. When the M4 probe was incubated and electrophoresed with nuclear extracts containing wild type AML1 in the presence of PEBP2β, a distinct band was observed that was not recognized in the lane loaded with the mock transfectant (Fig. 5*C*, *left*, *lanes 1* and *2*). This band became undetectable when a cold probe was coincubated with a labeled probe (*lane 3*), indicating that it represents a specific AML1-DNA complex. We again found that DNA binding of K24R/K43R was significantly reduced, although it still remained at a detectable level. Immunoblot analysis of nuclear extracts confirmed the presence of equal amounts of the AML1 proteins in all samples (Fig. 5*C*, *right*). Taken as a whole, these results demonstrated that DNA binding of AML1 could be regulated by acetylation of Lys-24 and Lys-43.

Heterodimerization with PEBP2β Is Not Modulated by Acetylation of AML1—The affinity of AML1 for DNA is markedly increased by heterodimerization through the Runt domain with PEBP2β, which could not interact with DNA by itself (10–13). It is possible that the altered interaction with PEBP2β could determine the DNA binding property of acetylated AML1. We asked, therefore, whether mutation of Lys-24 and Lys-43 in AML1 affects the interaction with PEBP2β. COS7 cells were transfected with wild type AML1, K24R/K43R, or K24A/K43A together with PEBP2β. The cells were lysed and immunoprecipitated with anti-PST and then subjected to immunoblot analysis using anti-PEBP2β. As shown in Fig. 6*A*, K24R/K43R and K24A/K43A associated with PEBP2β as effectively as wild type AML1. The expression level of each construct was confirmed by immunoblotting of whole cell lysates. These data indicate that Lys-24 and Lys-43, the target residues for acetylation, are dispensable for heterodimerization between AML1 and PEBP2β, suggesting that acetylation of AML1 does not affect the affinity for PEBP2β.

Acetylation by p300 Stimulates Transcriptional Activation of AML1—Because DNA binding of AML1 is stimulated in an acetylation-dependent manner, it is tempting to speculate that the transcriptional activity of AML1 can potentially be regulated by acetylation. To determine this, we examined whether substitution of Lys-24 and Lys-43 could modify transcriptional responses induced by AML1. For these experiments, we employed a reporter plasmid pM-CSF-R-luc in which the M-CSF receptor promoter is linked to the luciferase gene because it is efficiently activated by exogenous expression of AML1 (29). Wild type AML1, K24R/K43R, or K24A/K43A was introduced into HeLa cells, which lack endogenous AML1 activity, together with the reporter plasmid, and then luciferase activities were evaluated. As shown in Fig. 6*B*, we observed a 7-fold activation of pM-CSF-R-luc when wild type AML1 was expressed. In contrast, both K24R/K43R and K24A/K43A showed a significantly reduced transcriptional activation. Although p300 expression further enhanced the transcriptional activity of wild type AML1, impaired transcription by K24R/K43R and K24A/K43A was not restored even in the presence of p300. We confirmed that both K24R/K43R and K24A/K43A were ex-

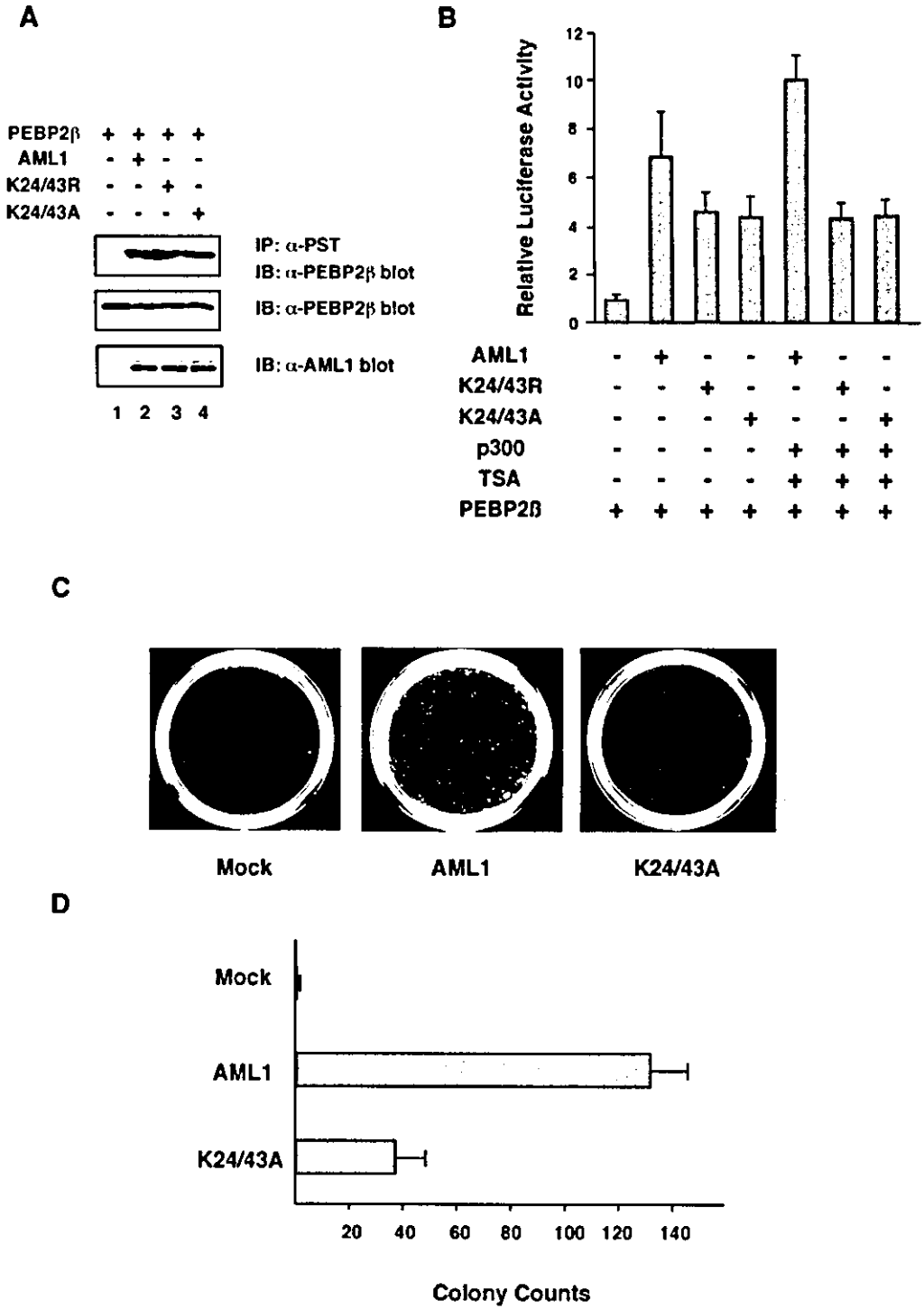

FIG. 6. *A*, interactions of wild type and the lysine mutant of AML1 with PEBP2β. COS7 cells were transfected with pME18S, wild type AML1, K24R/K43R, or K24A/K43A, together with PEBP2β as indicated. Cells were lysed, immunoprecipitated (*IP*) with anti-PST, and subjected to immunoblotting (*IB*) with anti-PEBP2β (*top*). Expression of each protein is monitored by immunoblotting of whole cell lysates with either anti-PEBP2β or anti-AML1 (*middle* and *bottom*). *B*, acetylation of AML1 stimulates its transcriptional activity. pM-CSF-R-luc was co-transfected into HeLa cells with each set of expression plasmids either with or without co-expression of p300, and the cells were analyzed for luciferase activity. Trichostatin A was added where indicated to a final concentration of 50 ng/ml at 8 h prior to harvest. Values of the relative luciferase activity and *error bars* represent the means and the standard deviations, respectively, for three independent experiments. *C*, soft agar assays with NIH3T3 cells expressing AML1 and the K24A/K43A mutant. NIH3T3 cells infected with retroviruses for AML1 or K24A/K43A of a comparable titer were seeded in soft agar after G418 selection and cultured for 14 days. Cells infected with AML1 gave larger average colony sizes and increased colony numbers, whereas cells infected with K24A/K43A created barely macroscopic colonies in agar as well as mock-infected (*mock*) cells. *D*, comparison of transforming activities of AML1 and K24A/K43A. Colonies greater than 0.25 mm in diameter were counted as positive. *Numbers* and *error bars* show the means and standard deviations of colony counts, respectively, for three independent experiments.

pressed as efficiently as wild type AML1 in HeLa cells (data not shown). These data strongly suggest that p300-mediated acetylation of AML1 on Lys-24 and Lys-43 is required for the optimal transcriptional activation of AML1.

Disruption of the Target Lysines Impairs Fibroblast-transforming Activity of AML1—Previously, we reported that overexpression of AML1 induces neoplastic transformation of NIH3T3 cells depending on the DNA binding ability and the

transcriptional activity (19). Furthermore, functional modulation of AML1 such as ERK-dependent phosphorylation significantly alters the transforming activity of AML1 (34). To study a role of acetylation in the *in vivo* function of AML1, we compared transforming activities of the wild type and the lysine mutant of AML1. Replication-deficient retroviruses for AML1 and K24A/K43A were generated by hyperexpression of the corresponding plasmid in COS7 cells. NIH3T3 cells were infected with these retroviruses, and soft agar assays were performed on G418-resistant populations. As shown in Fig. 6, *C* and *D*, wild type AML1 rapidly produced a number of macroscopic colonies in soft agar. In contrast, replacement of Lys-24 and Lys-43 to alanines remarkably impaired the transforming activity of AML1, presumably because of the inability to bind to DNA efficiently. AML1 and K24A/K43A showed equivalent expression levels in NIH3T3 cells (data not shown). These results suggest that p300-mediated acetylation on Lys-24 and Lys-43 is also important for the biological activity of AML1 *in vivo*.

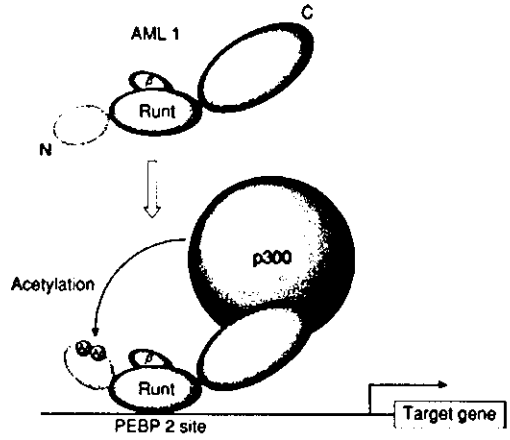

FIG. 7. **Schematic model for a regulatory mechanism of AML1 acetylation.** Physical interaction with p300 induces acetylation of AML1 at the two lysine residues in NRDBn, leading to the increase in DNA binding and transcriptional activation. NRDBn is a negative regulatory region for DNA binding N-terminal to the Runt domain.

DISCUSSION

In this study, we showed that AML1 interacts with p300 and is acetylated on the two conserved lysines in the N terminus adjacent to the Runt domain. Acetylation increases sequence-specific DNA binding of AML1 and is needed for efficient transcriptional activation by AML1. Furthermore, acetylation plays a key role for the transforming activity of AML1 in fibroblasts.

Acetylation of proteins is shown to have both stimulatory and inhibitory effects on transcription (54, 55). As for histones, acetylation is reversible and affects the strength of protein-DNA or protein-protein interactions. In addition, acetylation of several transcription factors, such as p53 and MyoD, enhances transcription of their target genes (56, 57). In contrast, acetylation of *Drosophila* T-cell receptor, high mobility group protein I/Y, and activator of thyroid and retinoic acid receptor results in decreased transcription (58–60). Thus, acetylation plays bipartite roles in the regulation of gene expression. Recently, it was reported that acetylation of E2F enhances its function via multiple mechanisms including protein half-life other than the increased DNA binding activity and transcriptional activation. These findings suggest that acetylation may affect transcription factors at multiple steps (61). In the present case, one can envision several models for the regulatory mechanisms of AML1 by acetylation. First, p300-mediated acetylation may stabilize AML1 through a prolonged protein half-life. However, we could not observe that mutation of Lys-24 and Lys-43 causes a significant difference in protein stabilization when compared with wild type (Fig. 4). Secondly, acetylation may directly increase the affinity of AML1 for DNA. Significant in this regard is our demonstration that the residues of AML1 acetylated by p300 are located in the negative regulatory region for DNA binding N-terminal to the Runt domain (NRDBn) (25, 62). It might be expected that acetylation could induce a conformational change in NRDBn that unmasks the DNA-binding interface of the Runt domain, resulting in potentiation of sequence-specific DNA binding. Schematic model for this hypothesis is shown in Fig. 7. However, Gu *et al.* (63) reported the controversial results that sequences N-terminal to the Runt domain do not affect DNA binding, which does not support this hypothesis. Another possibility is that acetylation may cause an increase in heterodimerization of AML1 with PEBP2β (25, 62). However, substitution of Lys-24 and Lys-43 does not affect the affinity of AML1 to PEBP2β, indicating that acetylation of AML1 does not contribute to heterodimerization with PEBP2β (Fig. 6*A*). Therefore, the increase in DNA binding by p300-mediated acetylation would reflect the altered interaction of AML1 itself with DNA rather than the lack of enhancing effect of the β protein. Finally, acetylation could affect protein-protein interactions, as described for binding of histone tails to the yeast transcriptional repressor Tup1 (64). Along these lines, further studies are in progress to elucidate the effect of AML1 acetylation on binding to other transcription factors such as Ets-1, CCAAT/enhancer binding protein-α, and PU.1.

In contrast to the remarkable effect of p300 acetylation on DNA binding of AML1, an impact on the transcriptional activation is relatively small. This discrepancy could be explained in several ways. First, AML1 manifests its transcriptional activation by participating in the assembly of a high order enhancer complex including other transcription factors as described above. These proteins in the complex may partially compensate for the decrease in DNA binding of AML1, which prevents a total loss of transcriptional activation. In this regard, it should be noticed that DNA binding of AML1 K24R/K43R can be detected to some extent in EMSA using nuclear extracts of COS7 cells, whereas it is much less detectable in EMSA using recombinant proteins (Fig. 5). Since many cooperating factors that associate with AML1 are supposed to exist in the nuclear extracts in contrast to highly purified recombinant proteins, it is reasonable to speculate that the formation of such a complex can partially compensate for decrease in DNA binding of AML1, which may blunt the effect of AML1 acetylation in transcriptional responses. Further investigation is needed to determine the existence of other possible intermolecular interactions. Another possibility is that other functional modifications of AML1, such as phosphorylation and methylation, may dampen the consequence of acetylation in transcriptional responses. In particular, phosphorylation is a critical modification that regulates the DNA binding activity, nuclear localization, protein interaction, and transactivation of various transcription factors. For example, p53 is phosphorylated in response to DNA damage, leading to stabilization and stimulated DNA binding *in vitro* (65, 66). Acetylation of C terminus of p53 is also observed in response to DNA damage. Furthermore, C-terminal acetylation of p53 has been shown to be regulated through its N-terminal phosphorylation induced by DNA damage, indicating an intimate cascade between phosphorylation and acetylation (56, 67, 68). Previously, we demonstrated that transcriptional activation of AML1 is regulated through phosphorylation by ERK at the specific serine residues (Ser-246 and Ser-266). Phosphorylation of AML1 is induced by cytokine stimulation in hematopoietic cells. Taken together with our present studies, it is now clear that AML1 undergoes

two types of posttranslational modifications (Fig. 7). A potential association between phosphorylation and acetylation of AML1 remains to be further investigated.

Acknowledgments—We thank M. Ohki for the gift of the human AML1 cDNAs, D. Zhang for providing the pM-CSF-R-luc vector, and Owen N Witte for the pSRαMSVtk*neo* vector and the helper virus plasmid. We also thank K. Miyazono and M. Kawabata for providing pcDEF3-p300.

REFERENCES

1. Rubnitz, J. E., and Look, A. T. (1998) *Curr. Opin. Hematol.* **5,** 264–270
2. Erickson, P., Gao, J., Chang, K. S., Look, T., Whisenant, E., Raimondi, S., Lasher, R., Trujillo, J., Rowley, J., and Drabkin, H. (1992) *Blood* **80,** 1825–1831
3. Miyoshi, H., Shimizu, K., Kozu, T., Maseki, N., Kaneko, Y., and Ohki, M. (1991) *Proc. Natl. Acad. Sci. U. S. A.* **88,** 10431–10434
4. Nisson, P. E., Watkins, P. C., and Sacchi, N. (1993) *Cancer Genet. Cytogenet.* **66,** 81
5. Mitani, K., Ogawa, S., Tanaka, T., Miyoshi, H., Kurokawa, M., Mano, H., Yazaki, Y., Ohki, M., and Hirai, H. (1994) *EMBO J.* **13,** 504–510
6. Nucifora, G., and Rowley, J. D. (1995) *Blood* **86,** 1–14
7. Romana, S. P., Mauchauffe, M., Le Coniat, M., Chumakov, I., Le Paslier, D., Berger, R., and Bernard, O. A. (1995) *Blood* **85,** 3662–3670
8. Shurtleff, S. A., Buijs, A., Behm, F. G., Rubnitz, J. E., Raimondi, S. C., Hancock, M. L., Chan, G. C., Pui, C. H., Grosveld, G., and Downing, J. R. (1995) *Leukemia (Basingstoke)* **9,** 1985–1989
9. Kania, M. A., Bonner, A. S., Duffy, J. B., and Gergen, J. P. (1990) *Genes Dev.* **4,** 1701–1713
10. Kagoshima, H., Shigesada, K., Satake, M., Ito, Y., Miyoshi, H., Ohki, M., Pepling, M., and Gergen, P. (1993) *Trends Genet.* **9,** 338–341
11. Meyers, S., Downing, J. R., and Hiebert, S. W. (1993) *Mol. Cell. Biol.* **13,** 6336–6345
12. Ogawa, E., Maruyama, M., Kagoshima, H., Inuzuka, M., Lu, J., Satake, M., Shigesada, K., and Ito, Y. (1993) *Proc. Natl. Acad. Sci. U. S. A.* **90,** 6859–6863
13. Wang, S., Wang, Q., Crute, B. E., Melnikova, I. N., Keller, S. R., and Speck, N. A. (1993) *Mol. Cell. Biol.* **13,** 3324–3339
14. Lutterbach, B., and Hiebert, S. W. (2000) *Gene (Amst.)* **245,** 223–235
15. Speck, N. A., and Terryl, S. (1995) *Crit. Rev. Eukaryotic Gene Expression* **5,** 337–364
16. Okuda, T., van Deursen, J., Hiebert, S. W., Grosveld, G., and Downing, J. R. (1996) *Cell* **84,** 321–330
17. Wang, Q., Stacy, T., Binder, M., Marin-Padilla, M., Sharpe, A. H., and Speck, N. A. (1996) *Proc. Natl. Acad. Sci. U. S. A.* **93,** 3444–3449
18. Wang, Q., Stacy, T., Miller, J. D., Lewis, A. F., Gu, T. L., Huang, X., Bushweller, J. H., Bories, J. C., Alt, F. W., Ryan, G., Liu, P. P., Wynshaw-Boris, A., Binder, M., Marin-Padilla, M., Sharpe, A. H., and Speck, N. A. (1996) *Cell* **87,** 697–708
19. Kurokawa, M., Tanaka, T., Tanaka, K., Ogawa, S., Mitani, K., Yazaki, Y., and Hirai, H. (1996) *Oncogene* **12,** 883–892
20. Miyoshi, H., Ohira, M., Shimizu, K., Mitani, K., Hirai, H., Imai, T., Yokoyama, K., Soeda, E., and Ohki, M. (1995) *Nucleic Acids Res.* **23,** 2762–2769
21. Zhang, Y. W., Bae, S. C., Huang, G., Fu, Y. X., Lu, J., Ahn, M. Y., Kanno, Y., Kanno, T., and Ito, Y. (1997) *Mol. Cell. Biol.* **17,** 4133–4145
22. Meyers, S., Lenny, N., and Hiebert, S. W. (1995) *Mol. Cell. Biol.* **15,** 1974–1982
23. Kitabayashi, I., Yokoyama, A., Shimizu, K., and Ohki, M. (1998) *EMBO J.* **17,** 2994–3004
24. Hernandez-Munain, C., and Krangel, M. S. (1995) *Mol. Cell. Biol.* **15,** 3090–3099
25. Kim, W. Y., Sieweke, M., Ogawa, E., Wee, H. J., Englmeier, U., Graf, T., and Ito, Y. (1999) *EMBO J.* **18,** 1609–1620
26. Selvamurugan, N., Chou, W. Y., Pearman, A. T., Pulumati, M. R., and Partridge, N. C. (1998) *J. Biol. Chem.* **273,** 10647–10657
27. Tenen, D. G., Hromas, R., Licht, J. D., and Zhang, D. E. (1997) *Blood* **90,** 489–519
28. Wotton, D., Ghysdael, J., Wang, S., Speck, N. A., and Owen, M. J. (1994) *Mol. Cell. Biol.* **14,** 840–850
29. Zhang, D. E., Hetherington, C. J., Meyers, S., Rhoades, K. L., Larson, C. J., Chen, H. M., Hiebert, S. W., and Tenen, D. G. (1996) *Mol. Cell. Biol.* **16,** 1231–1240
30. Zhang, D. E., Hohaus, S., Voso, M. T., Chen, H. M., Smith, L. T., Hetherington, C. J., and Tenen, D. G. (1996) *Curr. Top. Microbiol. Immunol.* **211,** 137–147
31. Aronson, B. D., Fisher, A. L., Blechman, K., Caudy, M., and Gergen, J. P. (1997) *Mol. Cell. Biol.* **17,** 5581–5587
32. Imai, Y., Kurokawa, M., Tanaka, K., Friedman, A. D., Ogawa, S., Mitani, K., Yazaki, Y., and Hirai, H. (1998) *Biochem. Biophys. Res. Commun.* **252,** 582–589
33. Lutterbach, B., Westendorf, J. J., Linggi, B., Isaac, S., Seto, E., and Hiebert, S. W. (2000) *J. Biol. Chem.* **275,** 651–656
34. Tanaka, T., Kurokawa, M., Ueki, K., Tanaka, K., Imai, Y., Mitani, K., Okazaki, K., Sagata, N., Yazaki, Y., Shibata, Y., Kadowaki, T., and Hirai, H. (1996) *Mol. Cell. Biol.* **16,** 3967–3979
35. Imai, Y., Kurokawa, M., Yamaguchi, Y., Izutsu, K., Nitta, E., Mitani, K., Satake, M., Noda, T., Ito, Y., and Hirai, H. (2004) *Mol. Cell. Biol.* **24,** 1033–1043
36. Bannister, A. J., and Kouzarides, T. (1996) *Nature* **384,** 641–643
37. Ogryzko, V. V., Schiltz, R. L., Russanova, V., Howard, B. H., and Nakatani, Y. (1996) *Cell* **87,** 953–959
38. Goodman, R. H., and Smolik, S. (2000) *Genes Dev.* **14,** 1553–1577
39. Turner, B. M. (1998) *CMLS Cell Mol. Life Sci.* **54,** 21–31
40. Bannister, A. J., and Miska, E. A. (2000) *CMLS Cell Mol. Life Sci.* **57,** 1184–1192
41. Chen, H., Tini, M., and Evans, R. M. (2001) *Curr. Opin. Cell. Biol.* **13,** 218–224
42. Sterner, D. E., and Berger, S. L. (2000) *Microbiol. Mol. Biol. Rev.* **64,** 435–459
43. Tanaka, K., Tanaka, T., Kurokawa, M., Imai, Y., Ogawa, S., Mitani, K., Yazaki, Y., and Hirai, H. (1998) *Blood* **91,** 1688–1699
44. Yamagata, T., Mitani, K., Oda, H., Suzuki, T., Honda, H., Asai, T., Maki, K., Nakamoto, T., and Hirai, H. (2000) *EMBO J.* **19,** 4676–4687
45. Tanaka, T., Tanaka, K., Ogawa, S., Kurokawa, M., Mitani, K., Nishida, J., Shibata, Y., Yazaki, Y., and Hirai, H. (1995) *EMBO J.* **14,** 341–350
46. Kunkel, T. A., Roberts, J. D., and Zakour, R. A. (1987) *Methods Enzymol.* **154,** 367–382
47. Zhang, D. E., Hetherington, C. J., Chen, H. M., and Tenen, D. G. (1994) *Mol. Cell. Biol.* **14,** 373–381
48. Tanaka, T., Mitani, K., Kurokawa, M., Ogawa, S., Tanaka, K., Nishida, J., Yazaki, Y., Shibata, Y., and Hirai, H. (1995) *Mol. Cell. Biol.* **15,** 2383–2392
49. Tanaka, K., Tanaka, T., Ogawa, S., Kurokawa, M., Mitani, K., Yazaki, Y., and Hirai, H. (1995) *Biochem. Biophys. Res. Commun.* **211,** 1023–1030
50. Furukawa, K., Yamaguchi, Y., Ogawa, E., Shigesada, K., Satake, M., and Ito, Y. (1990) *Cell Growth & Differ.* **1,** 135–147
51. Tanaka, T., Nishida, J., Mitani, K., Ogawa, S., Yazaki, Y., and Hirai, H. (1994) *J. Biol. Chem.* **269,** 24020–24026
52. Kurokawa, M., Ogawa, S., Tanaka, T., Mitani, K., Yazaki, Y., Witte, O. N., and Hirai, H. (1995) *Oncogene* **11,** 833–840
53. Martin, D. I., and Orkin, S. H. (1990) *Genes Dev.* **4,** 1886–1898
54. Imhof, A., Yang, X. J., Ogryzko, V. V., Nakatani, Y., Wolffe, A. P., and Ge, H. (1997) *Curr. Biol.* **7,** 689–692
55. Korzus, E., Torchia, J., Rose, D. W., Xu, L., Kurokawa, R., McInerney, E. M., Mullen, T. M., Glass, C. K., and Rosenfeld, M. G. (1998) *Science* **279,** 703–707
56. Sakaguchi, K., Herrera, J. E., Saito, S., Miki, T., Bustin, M., Vassilev, A., Anderson, C. W., and Appella, E. (1998) *Genes Dev.* **12,** 2831–2841
57. Sartorelli, V., Puri, P. L., Hamamori, Y., Ogryzko, V., Chung, G., Nakatani, Y., Wang, J. Y., and Kedes, L. (1999) *Mol. Cell* **4,** 725–734
58. Chakravarti, D., Ogryzko, V., Kao, H. Y., Nash, A., Chen, H., Nakatani, Y., and Evans, R. M. (1999) *Cell* **96,** 393–403
59. Munshi, N., Merika, M., Yie, J., Senger, K., Chen, G., and Thanos, D. (1998) *Mol. Cell* **2,** 457–467
60. Waltzer, L., and Bienz, M. (1998) *Nature* **395,** 521–525
61. Martinez-Balbas, M. A., Bauer, U. M., Nielsen, S. J., Brehm, A., and Kouzarides, T. (2000) *EMBO J.* **19,** 662–671
62. Ito, Y. (1999) *Genes Cells* **4,** 685–696
63. Gu, T. L., Goetz, T. L., Graves, B. J., and Speck, N. A. (2000) *Mol. Cell. Biol.* **20,** 91–103
64. Edmondson, D. G., Smith, M. M., and Roth, S. Y. (1996) *Genes Dev.* **10,** 1247–1259
65. Meek, D. W. (1998) *Cell. Signal* **10,** 159–166
66. Prives, C., and Hall, P. A. (1999) *J. Pathol.* **187,** 112–126
67. Liu, L., Scolnick, D. M., Trievel, R. C., Zhang, H. B., Marmorstein, R., Halazonetis, T. D., and Berger, S. L. (1999) *Mol. Cell. Biol.* **19,** 1202–1209
68. Luo, J., Su, F., Chen, D., Shiloh, A., and Gu, W. (2000) *Nature* **408,** 377–381

Bone Marrow Transplantation (2004) 33, 549–552

www.nature.com/bmt

Graft-versus-host disease

Increased incidence of acute graft-versus-host disease with the continuous infusion of cyclosporine A compared to twice-daily infusion

N Ogawa, Y Kanda, M Matsubara, Y Asano, M Nakagawa, M Sakata-Yanagimoto, K Kandabashi, K Izutsu, Y Imai, A Hangaishi, M Kurokawa, S Tsujino, S Ogawa, K Aoki, S Chiba, T Motokura and H Hirai

Department of Cell Therapy and Transplantation Medicine, University of Tokyo, Bunkyo-ku, Tokyo, Japan

Summary:

We retrospectively compared the incidence of acute graft-versus-host disease (GVHD) before and after September 1999, when we changed the mode of cyclosporine A (CsA) administration from twice-daily infusions (TD) ($n = 58$) to continuous infusion (CIF) ($n = 71$). The incidence of grade II–IV acute GVHD in the CIF group (56%) was significantly higher than that in the TD group (27%, $P = 0.00022$). Multivariate analysis identified only two independent significant risk factors for the development of grade II–IV acute GVHD; CIF of CsA (relative risk 2.59, 95% CI 1.46–4.60, $P = 0.0011$) and the presence of HLA mismatch (2.01, 95% CI 1.15–3.53, $P = 0.014$). The incidence of relapse was significantly lower in the CIF group when adjusted for disease status before transplantation (0.41, 95% CI 0.18–0.95, $P = 0.038$), which resulted in better disease-free survival in high-risk patients (43 *vs* 16% at 2 years, $P = 0.039$), but not in standard-risk patients (72 *vs* 80%, $P = 0.45$). CIF of CsA with a target level of 250–400 ng/ml may not be appropriate for GVHD prophylaxis in standard-risk patients.

Bone Marrow Transplantation (2004) **33**, 549–552. doi:10.1038/sj.bmt.1704374
Published online 12 January 2004
Keywords: hematopoietic stem cell transplantation; cyclosporine A; graft-versus-host disease; continuous infusion

Cyclosporine A (CsA) is a mainstay of treatment in the pharmacologic prevention of graft-versus-host disease (GVHD), and is usually combined with methotrexate (MTX). However, the dose, target blood level, and schedule of administration vary among protocols.[1] In particular, it has not been assessed whether CsA should be administered as a continuous infusion (CIF) or as twice-daily infusions (TD) in the early period after transplantation when patients cannot tolerate an oral intake. In September 1999, we changed the mode of CsA administration from TD to CIF, without major changes to other transplantation procedures. The aim of this study was to evaluate the impact of these two different modes of administration on the incidence of acute GVHD.

Correspondence: Dr Y Kanda, Department of Cell Therapy and Transplantation Medicine, University of Tokyo, 7-3-1 Hongo, Bunkyo-ku, Tokyo 113-8655, Japan; E-mail: ycanda@umin.ac.jp
Received 09 April 2003; accepted 05 July 2003
Published online 12 January 2004

Patients and methods

Patients

We retrospectively analyzed the records of adult patients who underwent allogeneic hematopoietic stem cell transplantation for the first time between June 1995 and May 2000 using a GVHD prophylaxis regimen consisting of CsA and MTX. During that time, this combination was the standard regimen for GVHD prophylaxis in our center, but CsA alone was used for patients who were at a very high risk for relapse, and a combination of tacrolimus and MTX was used for patients who had received a graft from an unrelated donor with at least one allele or antigen mismatch. Those who received a T-cell-depleted graft and those who received a reduced-intensity conditioning regimen or a conditioning regimen that included ATG or CAMPATH1-H were excluded. Otherwise, consecutive patients were included in the study. The data for 129 patients were analyzed. There were 95 males and 34 females with a median age of 38 years (range 18–60). Bone marrow (BM) was exclusively used in unrelated transplants, whereas 13 related donors chose a collection of G-CSF-mobilized peripheral blood stem cells (PBSC) rather than a BM harvest. BM was additionally harvested from poor mobilizers.

Transplantation procedure

Conditioning was mainly a combination of cyclophosphamide (60 mg/kg for 2 days) with either busulfan (4 mg/kg/day for 4 days) or total body irradiation (TBI; 2 Gy twice daily for 3 days). GVHD prophylaxis was with CsA and short-term MTX (10–15 mg/m^2 on day 1 and 7–10 mg/m^2 on days 3 and 6, and optionally on day 11), with a starting dose of CsA of 3 mg/kg/day. Before September 1999, CsA was administered as a 4 h infusion twice daily in equally divided doses. The dose of CsA was adjusted to maintain the trough blood CsA concentration between 150

and 300 ng/ml. After September 1999, CsA was administered as a CIF. The dose of CsA was adjusted to maintain the blood CsA concentration between 250 and 400 ng/ml. CsA concentration was measured at least once a week by fluorescence polarization immunoassay with a specific monoclonal antibody, using whole blood samples.[2] Metabolites of CsA were not measured by this method. The route of CsA administration was converted to oral at a ratio of 1:2 or 1:3 when patients were able to tolerate oral intake at least 3 weeks after transplantation. Acute GVHD was graded as previously described.[3] Prophylaxis against bacterial, fungal, and pneumocystis carinii infection consisted of fluconazole, tosufloxacin, and sulfamethoxazole/trimethoprim. As prophylaxis against herpes simplex virus infection, acyclovir was given from day −7 to 35. Pre-emptive therapy for cytomegalovirus infection was with ganciclovir, while monitoring cytomegalovirus antigenemia.[4]

Statistical considerations

Standard-risk disease was defined as acute leukemia in complete remission, chronic myelocytic leukemia in the first chronic phase, chemosensitive lymphoma, and myelodysplastic syndrome comprising refractory anemia or refractory anemia with ringed sideroblasts, while others were considered high-risk diseases. Renal dysfunction was defined as an elevation in serum creatinine level to above $\times 1.5$ or $\times 2.0$ the baseline value, except for that clearly caused by the administration of amphotericin B. Patients who received both BM and PBSC grafts were included in the PBSC group.

Probabilities and continuous variables in the two groups were compared using Fisher's exact test and the Mann–Whitney *U*-test, respectively. Cumulative incidences of acute GVHD and relapse were calculated using Gray's method, considering death without acute GVHD or relapse, as a competing risk.[5] Disease-free survival was estimated using the Kaplan–Meier method. Potential confounding factors considered in the analysis were age, sex, donor type (related or unrelated), stem cell source (BM or PBSC), disease risk, conditioning regimen, HLA mismatch, total dose of MTX, and mode of CsA administration.

Results

Patient characteristics

Of the 129 patients analyzed, 58 and 71 patients were in the TD and CIF groups, respectively. The CIF group included a significantly higher proportion of patients with high-risk disease ($P=0.021$), those transplanted from an unrelated donor ($P=0.004$), those who received an HLA-mismatched graft ($P=0.023$), and those who received a PBSC graft ($P=0.0061$) (Table 1). The total dose of MTX was significantly lower in the CIF group (median dose 35 mg/m^2 *vs* 33 mg/m^2, $P=0.0002$). Other characteristics were equivalent between the two groups.

Risk factors for grade II–IV acute GVHD

First, we performed a univariate analysis to evaluate the impact of potential confounding factors on the incidence of grade II–IV acute GVHD. As shown in Table 2, transplant from an unrelated donor, the presence of HLA mismatch, the use of a TBI-containing regimen, a lower total dose of MTX, and CIF of CsA were identified as significant risk factors for the development of grade II–IV acute GVHD. The incidence of grade II–IV acute GVHD in the CIF group (56%) was significantly higher than that in the TD group (27%, $P=0.00022$, Figure 1). Next, we performed a multivariate analysis using the backward stepwise selection method to identify independent risk factors for the development of grade II–IV acute GVHD. Only two factors, CIF of CsA (relative risk 2.59; 95% CI 1.46–4.60, $P=0.0011$) and the presence of HLA mismatch (2.01; 95% CI 1.15–3.53, $P=0.014$), were identified as independent significant risk factors (Table 3A). The impact of these two factors was significant even when adjusted for the total dose of MTX and donor type (Table 3B).

Table 1 Characteristics of the patients

	TD group (n=58)	*CIF group (n=71)*	*P-value*
Sex			
Male	42	53	0.84
Female	16	18	
Age			
<40 years	36	36	0.22
⩾40 years	22	35	
Risk			
Standard	39	33	0.021
High	19	38	
Donor			
Related	42	33	0.004
Unrelated	16	38	
HLA			
Match	50	9	0.023
Mismatch	8	22	
Stem-cell BM	57	59	0.0061
PBSC	1	12	
Regimen non-TBI	19	17	0.33
TBI	39	54	0.33

[a]BM = bone marrow, PBSC = peripheral blood stem cell, TBI = total body irradiation.

Renal toxicity

Renal dysfunction was significantly less frequent in the CIF group than the TD group: 27% *vs* 66% ($P<0.0001$) and 13% *vs* 41% ($P=0.0002$), when we defined renal dysfunction as an elevation of the serum creatinine level to above $\times 1.5$ and $\times 2.0$ the baseline value, respectively (Table 4).

Actual daily dose of CsA

We adjusted the dose of CsA to maintain the target blood level as described above. We compared the actual daily dose of CsA, excluding patients who were converted to oral administration. The actual daily dose of CsA in the CIF

Table 2 Impact of pretransplant factors on the incidence of acute GVHD by univariate analyses

	Incidence of acute GVHD	*P-value*
Sex		
Male	45%	0.55
Female	38%	
Age		
<40 years	44%	0.82
$\geqslant 40$ years	42%	
Risk		
Standard	37%	0.15
High	51%	
Donor		
Related	36%	0.014
Unrelated	54%	
HLA		
Match	37%	0.0026
Mismatch	63%	
Stem cell		
BM	42%	0.33
PBSC	55%	
Regimen		
Non-TBI	30%	0.041
TBI	48%	
MTX		
$<35\,mg/m^2$	60%	0.0025
$\geqslant 35\,mg/m^2$	36%	
CsA		
TD	27%	0.00022
CIF	56%	

BM = bone marrow, PBSC = peripheral blood stem cell, TBI = total body irradiation, MTX = methotrexate, CsA = cyclosporine A, TD = twice-daily infusion, CIF = continuous infusion.

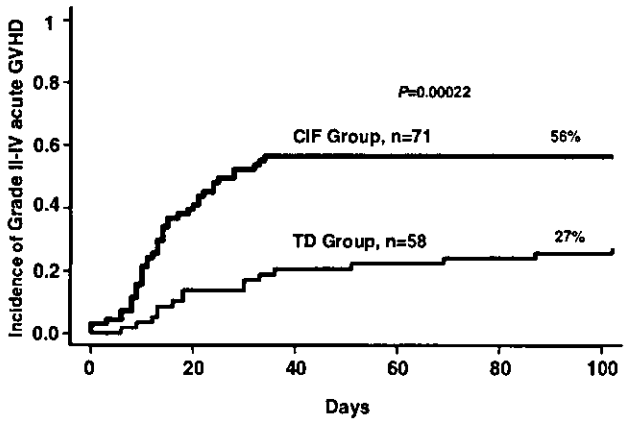

Figure 1 Cumulative incidence of grade II–IV acute GVHD grouped by the mode of CsA administration (TD = twice-daily infusion, CIF = contin-continuous infusion).

group was consistently significantly lower than that in the TD group during the first 4 weeks after transplantation (Figure 2).

Table 3 Impact of pretransplant factors on the incidence of acute GVHD by multivariate analysis: (a) independent significant risk factors identified by multivariate analysis using backward stepwise selection; (b) impact of HLA mismatch and the mode of cyclosporine A administration adjusted for the total methotrexate dose and the donor type (CsA = cyclosporine A, MTX = methotrexate, TD = twice-daily infusion, CIF = continuous infusion)

		Relative risk (95% CI)	*P-value*
	(A)		
HLA	Mismatch *vs* match	2.01 (1.15–3.53)	0.014
CsA	CIF *vs* TD	2.59 (1.46–4.60)	0.0011
	(B)		
HLA	Mismatch *vs* match	1.89 (1.04–3.45)	0.038
CsA	CIF *vs* TD	1.98 (0.98–4.00)	0.056
MTX	$\geqslant 35\,mg/m^2$ *vs* $<35\,mg/m^2$	1.51 (0.80–2.87)	0.20
Donor	Unrelated *vs* related	1.36 (0.78–2.38)	0.28

Table 4 Difference in the incidence of renal dysfunction by the mode of cyclosporine A administration (TD = twice-daily infusion, CIF = continuous infusion)

		(−)	*(+)*	*P-value*
Incidence of serum creatinine $>1.5\times$ *baseline value*				
CsA	TD	20	38 (66%)	<0.001
	CIF	52	19 (27%)	
Incidence of serum creatinine $>2.0\times$ *baseline value*				
CsA	TD	34	24 (40%)	0.0002
	CIF	62	9 (13%)	

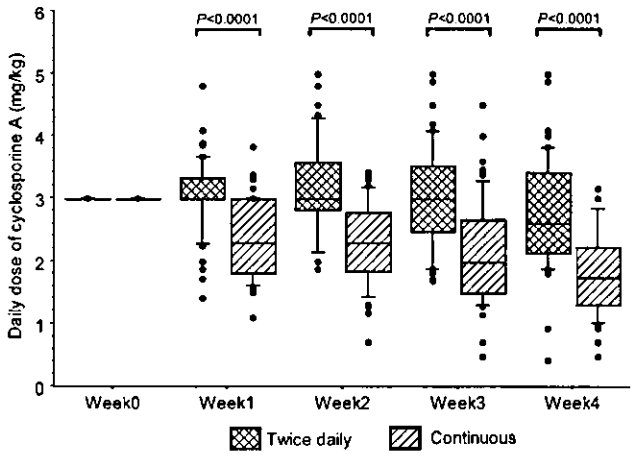

Figure 2 Actual daily dose of CsA grouped by the mode of administration. The box-and-whisker plot shows 10, 25, 50, 75, and 90 percentile values. Outliers are indicated by dots.

Transplant outcome

The CIF of CsA was shown to significantly decrease the incidence of relapse, after adjusting for disease status before transplantation (relative risk 0.41, 95% CI 0.18–0.95, $P = 0.038$). This resulted in significantly better disease-free

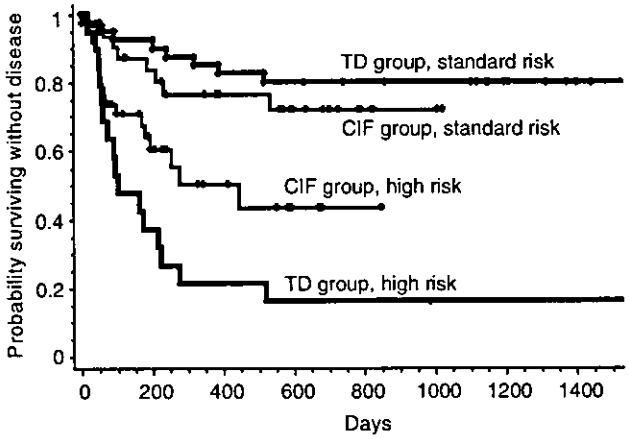

Figure 3 Disease-free survival grouped according to the mode of CsA administration, stratified by the disease status (TD = twice-daily infusion, CIF = continuous infusion).

survival in the CIF group than in the TD group among high-risk patients (43 *vs* 16% at 2 years, $P = 0.039$, Figure 3), whereas there was no significant difference in disease-free survival between the two groups among standard-risk patients (72 *vs* 80% at 2 years, $P = 0.45$).

Discussion

To summarize the findings of this study, the CIF of CsA with a target level of 250–400 ng/ml significantly increased the incidence of grade II–IV acute GVHD, but significantly decreased the incidences of renal dysfunction and relapse, which resulted in better disease-free survival in high-risk patients. However, disease-free survival was not improved in standard-risk patients, probably because the incidence of relapse was originally low in these patients. Therefore, this mode of CsA administration may not be appropriate for standard-risk patients.

There are at least two possible explanations for why the incidence of acute GVHD was higher in the CIF group. First, the total dose (or the area under the curve) of CsA may be important. Second, it may be important to achieve a peak CsA concentration. It was impossible to draw a definite conclusion from this study. However, considering that the actual daily dose of CsA was gradually decreased in the CIF group after transplantation, a target level of 250–400 ng/ml might be too low to prevent GVHD adequately, although this target level has been used in recent large randomized controlled trials.[6,7] Miller *et al*[8] adjusted the dose of CsA as a CIF to maintain the blood CsA level between 450 and 520 ng/ml. In this setting, the mean actual dose of CsA was maintained between 2.87 and 3.15 mg/kg during the first 4 weeks after transplantation. Therefore, this higher target level may be more appropriate when comparing the mode of CsA administration, although it needs to be confirmed by measuring the area under the curve.

The major shortcoming of this study was that this was not a randomized controlled trial and there were some uncontrolled variables that might have caused bias. However, the impact of the mode of CsA administration remained significant after adjusting for these uncontrolled variables, as shown in Table 3B. We are planning a randomized controlled trial to confirm these results.

Acknowledgements

This research was supported by a Grant-in-Aid for Scientific Research from the Ministry of Health, Labor and Welfare.

References

1 Ruutu T, Niederwieser D, Gratwohl A *et al.* A survey of the prophylaxis and treatment of acute GVHD in Europe: a report of the European Group for Blood and Marrow, Transplantation (EBMT). Chronic Leukaemia Working Party of the EBMT. *Bone Marrow Transplant* 1997; **19**: 759–764.
2 Alvarez JS, Sacristan JA, Alsar MJ. Comparison of a monoclonal antibody fluorescent polarization immunoassay with monoclonal antibody radioimmunoassay for cyclosporin determination in whole blood. *Ther Drug Monit* 1992; **14**: 78–80.
3 Thomas ED, Storb R, Clift RA *et al.* Bone-marrow transplantation (second of two parts). *N Engl J Med* 1975; **292**: 895–902.
4 Kanda Y, Mineishi S, Saito T *et al.* Pre-emptive therapy against cytomegalovirus (CMV) disease guided by CMV antigenemia assay after allogeneic hematopoietic stem cell transplantation: a single-center experience in Japan. *Bone Marrow Transplant* 2001; **27**: 437–444.
5 Gooley TA, Leisenring W, Crowley J *et al.* Estimation of failure probabilities in the presence of competing risks: new representations of old estimators. *Stat Med* 1999; **18**: 695–706.
6 Nash RA, Antin JH, Karanes C *et al.* Phase 3 study comparing methotrexate and tacrolimus with methotrexate and cyclosporine for prophylaxis of acute graft-versus-host disease after marrow transplantation from unrelated donors. *Blood* 2000; **96**: 2062–2068.
7 Ratanatharathorn V, Nash RA, Przepiorka D *et al.* Phase III study comparing methotrexate and tacrolimus (prograf, FK506) with methotrexate and cyclosporine for graft-versus-host disease prophylaxis after HLA-identical sibling bone marrow transplantation. *Blood* 1998; **92**: 2303–2314.
8 Miller KB, Schenkein DP, Comenzo R *et al.* Adjusted-dose continuous-infusion cyclosporin A to prevent graft-versus-host disease following allogeneic bone marrow transplantation. *Ann Hematol* 1994; **68**: 15–20.

nature medicine

AML-1 is required for megakaryocytic maturation and lymphocytic differentiation, but not for maintenance of hematopoietic stem cells in adult hematopoiesis

Motoshi Ichikawa[1,7], Takashi Asai[1,7], Toshiki Saito[1], Go Yamamoto[1], Sachiko Seo[1], Ieharu Yamazaki[3], Tetsuya Yamagata[1,5], Kinuko Mitani[4], Shigeru Chiba[1], Seishi Ogawa[1,2], Mineo Kurokawa[1] & Hisamaru Hirai[1,6]

Embryonic development of multilineage hematopoiesis requires the precisely regulated expression of lineage-specific transcription factors, including AML-1 (encoded by *Runx1*; also known as CBFA-2 or PEBP-2αB)[1–5]. *In vitro* studies and findings in human diseases, including leukemias[6,7], myelodysplastic syndromes[8] and familial platelet disorder with predisposition to acute myeloid leukemia (AML)[9], suggest that AML-1 has a pivotal role in adult hematopoiesis. However, this role has not been fully uncovered *in vivo* because of the embryonic lethality of *Runx1* knockout in mice. Here we assess the requirement of AML-1/*Runx1* in adult hematopoiesis using an inducible gene-targeting method[10]. In the absence of AML-1, hematopoietic progenitors were fully maintained with normal myeloid cell development. However, AML-1-deficient bone marrow showed inhibition of megakaryocytic maturation, increased hematopoietic progenitor cells and defective T- and B-lymphocyte development. AML-1 is thus required for maturation of megakaryocytes and differentiation of T and B cells, but not for maintenance of hematopoietic stem cells (HSCs) in adult hematopoiesis.

Using the Cre-*lox*P sequence-specific recombination system, we generated mutant mice in which exon 5 of the *Runx1* gene could be selectively deleted by the expression of Cre recombinase (Fig. 1a). We mated mutant animals carrying deleted (*Runx1*$^{-}$) or *lox*P-flanked (*Runx1*^{fl}) alleles, and observed lethal bleeding of *Runx1*$^{-/-}$ embryos as anticipated[1,2]. In contrast, *Runx1*$^{fl/fl}$ and *Runx1*$^{fl/-}$ mice were normal (data not shown). We then bred the mutant mice with *Mx-cre*-transgenic mice to generate *Runx1*$^{fl/+}$*Mx-cre* or *Runx1*$^{fl/-}$*Mx-cre* mice. In these mice, the *Runx1*^{fl} allele could be effectively deleted in hematopoietic progenitors by using injected polyinosinic-polycytidylic acid (pIpC) to induce expression of Cre recombinase[10]. Two months after pIpC injection, genomic Southern blot analysis of *Runx1*$^{fl/-}$*Mx-cre* mice revealed that ≥90% of the bone marrow or peritoneal exudative cells, ~80% of which were morphologically normal neutrophils, had biallelic *Runx1* deletion. This indicates that *Runx1* deletion was induced in most bone marrow cells, and that most myeloid progenitors lacking AML-1 could still differentiate into mature neutrophils (Fig. 1b,c). Efficient excision of one *Runx1* allele was observed in the hematopoietic cells, including lymphocytes, of *Runx1*$^{fl/+}$*Mx-cre* mice. In contrast, only 9%, 32% and 57% of the thymocytes, splenic T cells and B cells *of Runx1*$^{fl/-}$*Mx-cre* mice, respectively, had a *Runx1*$^{-/-}$ genotype. Therefore, a large proportion of mature lymphocytes originated from lymphoid progenitor cells still expressing intact AML-1, and AML-1 deficiency should be disadvantageous to lymphocyte development.

Injection of pIpC did not cause significant differences in neutrophil counts or hemoglobin levels among the *Runx1*$^{fl/-}$*Mx-cre* (floxed) mice, *Runx1*$^{fl/+}$*Mx-cre* mice and *Runx1*$^{+/+}$*Mx-cre* (control) mice (Fig. 2a). Immediately after pIpC injection, however, platelet counts for the floxed mice declined to one-third to one-sixth of those for the control mice (Fig. 2a). Lymphocyte counts were slightly depressed after more than 4 weeks in the floxed and *Runx1*$^{fl/+}$*Mx-cre* mice. These results suggest that AML-1 is required for the maintenance of platelets and lymphocytes, but not for the sustained production of erythrocytes and neutrophils.

We next examined bone marrow cell morphology in the pIpC-treated floxed mice to determine whether thrombocytopenia results from abnormal megakaryopoiesis. The cellularity of the bone marrow and morphology of myeloid cells in the floxed mice were not remarkably altered from those of the control mice, except for a slightly elevated myeloid-erythroid ratio (2.35 ± 0.70 in floxed mice compared with 1.71 ± 0.39 in control mice; $n = 7$ (paired), $P = 0.046$ by Wilcoxon signed-rank test; Fig. 2b and data not shown). However, Wright-Giemsa staining of floxed bone marrow revealed the absence of normal megakaryocytes with abundant cytoplasm and lobulated nuclei (Fig. 2b). Instead, the floxed bone marrow contained a small number of immature megakaryocyte-like cells with occasionally separated round nuclei,

[1]Department of Hematology and Oncology and [2]Department of Regeneration Medicine for Hematopoiesis, Graduate School of Medicine, University of Tokyo, 7-3-1 Hongo, Bunkyo-ku, Tokyo, 113-8655, Japan. [3]Department of Clinical Laboratory and Pathology, Inoue Memorial Hospital, 1-16 Shindencho, Chuo-ku, Chiba, 260-0027, Japan. [4]Department of Hematology, Dokkyo University School of Medicine, 800 Kitakobayashi, Mibu, Tochigi, 321-0293, Japan. [5]Present address: Immunology section, Joslin Diabetes Center, Harvard Medical School, One Joslin Place, Boston, Massachusetts 02215, USA. [6]Deceased. [7]These authors contributed equally to this work. Correspondence should be addressed to S.O. (sogawa-tky@umin.ac.jp).

Published online 15 February 2004; doi:10.1038/nm997

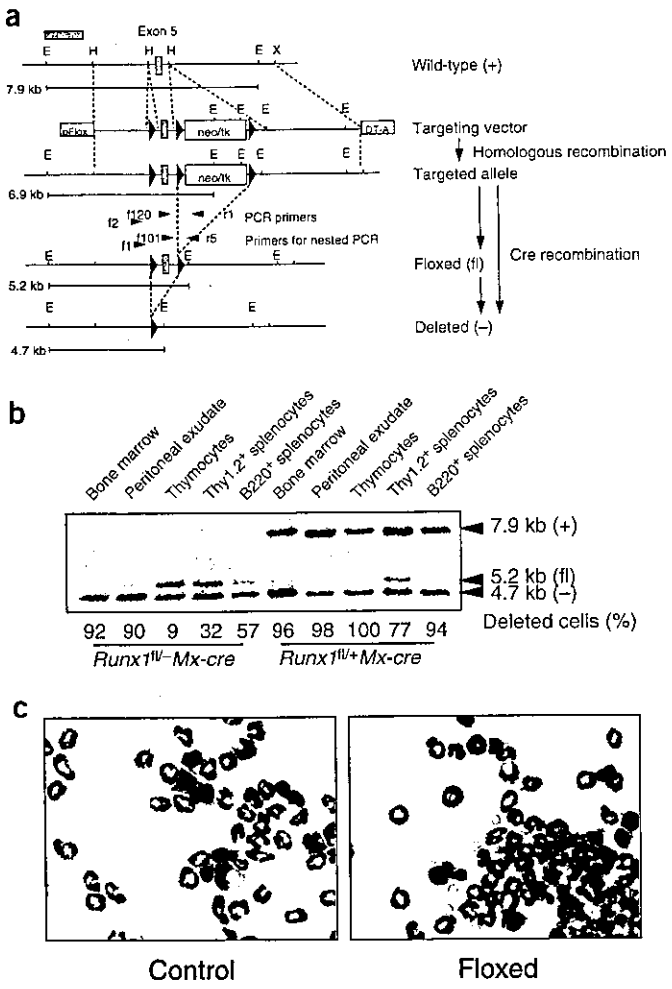

Figure 1 Inducible AML-1 knockout mice. (**a**) Schematic representation of conditional gene targeting of the *Runx1* gene. E, *Eco*RI; H, *Hin*dIII; X, *Xba*I; gray box in upper left corner, 5′ genomic probe; *neo/tk*, PGK-*neo*/HSV-thymidine kinase positive selection cassette; *DT-A*, diphtheria toxin A chain negative selection cassette. (**b**) Southern blot genotyping of cells from hematopoietic organs of mice injected with pIpC. Numbers below lanes indicate proportion of *Runx1*-deleted cells. (**c**) Wright-Giemsa-stained, cytocentrifuged specimens of peritoneal inflammatory cells genotyped in b.

resembling the abnormal 'micromegakaryocytes' observed in human myelodysplastic syndromes (Fig. 2b). Consistent with this observation, a substantial increase in the number of small megakaryocytes was revealed in the floxed bone marrow by acetylcholinesterase staining, which specifically detects mature and immature megakaryocytes[11] (Fig. 2b).

Given the prominent immaturity of megakaryocytes in the floxed mice, we examined the ultrastructure of the megakaryocytes (Fig. 2c). In addition to their smaller size, floxed megakaryocytes showed poorly developed demarcation membranes compared with megakaryocytes from control (*Runx1*$^{+/+}$*Mx-cre*) mice. During the maturation process, megakaryocytes acquire high DNA ploidy (>4*n*) through a cell cycle process known as endomitosis[12]. As expected from the smaller size of their nuclei, CD41^{+} megakaryocytes from the floxed mice showed a markedly lower level of polyploidy (≤8*n*) than megakaryocytes from the control mice (modal ploidy, 16*n*), as revealed by flow cytometric measurement of DNA content. This demonstrates that AML-1 deletion also causes defective polyploidization in megakaryocytes (Fig. 2d). Although a recent report showed that AML-1 regulates the expression of megakaryocyte-specific genes in cooperation with GATA-1 (ref. 13), and although the small and immature megakaryocytes that we observed are reminiscent of those found in GATA-1 knockdown mice[14,15], the expression levels of megakaryocyte-specific transcription factors in floxed mice, including GATA-1, FOG-1 and NF-E2, remained unaffected according to RT-PCR analyses of lineage-negative (Lin^{-}) bone marrow cells (data not shown).

We subsequently conducted *in vitro* colony-forming assays to evaluate the frequency of hematopoietic progenitors. Floxed bone marrow cells formed more megakaryocytic colonies (CFU-Meg) than control bone marrow cells in semisolid media (Fig. 3a). The numbers of myeloid and mixed (myeloid and erythroid) colonies were also elevated in the floxed bone marrow. Using single-colony PCR genotyping, we detected the *Runx1*$^{-/-}$ genotype in 149 of 150 myeloid colonies, 48 of 50 erythroid colonies, 35 of 36 mixed colonies and 14 of 14 megakaryocytic colonies from pIpC-treated floxed bone marrow cells, thus excluding the possibility that those hematopoietic cells might be predominantly derived from progenitor cells still expressing intact AML-1 (data not shown). Using flow cytometry (Fig. 3b), we observed an increased number of cells in the Lin-c-Kit^{hi}CD41^{hi} fraction, which was presumed to contain CFU-Meg[16], in the floxed bone marrow. Similarly, the number of cells defined by CD34-Lin$^{-/lo}$c-Kit^{hi}Sca-1^{hi} (Fig. 3c), which represent the most immature hematopoietic progenitor cell population[17], was also elevated in the floxed bone marrow. Although development of both T and B cells from AML-1-deficient cells was impaired (Fig. 1b), the cells defined by Lin$^{-/lo}$IL-7Rα^{+}Sca-1^{lo}c-Kit^{lo}, previously reported to include common lymphocyte progenitors (CLPs)[18], were maintained in the floxed bone marrow (Fig. 3d).

Increased numbers of primitive hematopoietic progenitors, immortalized myeloid progenitor cells and arrested myeloid maturation have been observed in mice expressing the leukemic AML-1/ETO chimeric protein[19–21], which dominantly suppresses the normal function of AML-1. We observed an elevated colony-replating capacity of *Runx1*$^{-/-}$ hematopoietic cells, although replating could be repeated for only 2 months (Fig. 3e). Although AML-1-null neutrophils were morphologically normal, and freshly collected floxed bone marrow cells did not show altered apoptosis when assessed by annexin-V expression (data not shown), we detected increased apoptosis of myeloid colony-forming cells, suggesting that a certain degree of maturation arrest occurs in the myeloid lineage in the absence of AML-1 (Fig. 3f).

Because immature hematopoietic progenitor cell fractions were elevated in the floxed bone marrow, we used a competitive repopulation assay to assess their ability to reconstitute adult hematopoiesis[22]. We used isotypes of the pan-hematopoietic marker CD45 (Ly5) to distinguish the origins of the repopulating cells. Sublethally irradiated C57BL/6-Ly5.1 recipient mice (Ly5.1^{+}Ly5.2^{-}) were intravenously injected with a mixture of bone marrow cells from C57BL/6-Ly5.1/Ly5.2 F_1 competitor mice (Ly5.1^{+}Ly5.2^{+}) or floxed or control mice (Ly5.1^{-}Ly5.2^{+}) previously injected with pIpC. We then analyzed Ly5 isotypes on the repopulating cells by flow cytometry (Fig. 4a). Notably, the floxed bone marrow cells reconstituted neither peripheral T (Thy-1.2^{+}) nor B (B220^{+}) cells, whereas there were no significant differences in the mature neutrophil (Gr-1^{hi}Mac-1^{+}) and monocyte populations (Gr-1^{lo}Mac-1^{+})[23] (Fig. 4a). The contribution to the reconstituted bone marrow was not significantly different in neutrophils (test/competitor = 0.382 ± 0.083 for floxed mice (*n* =

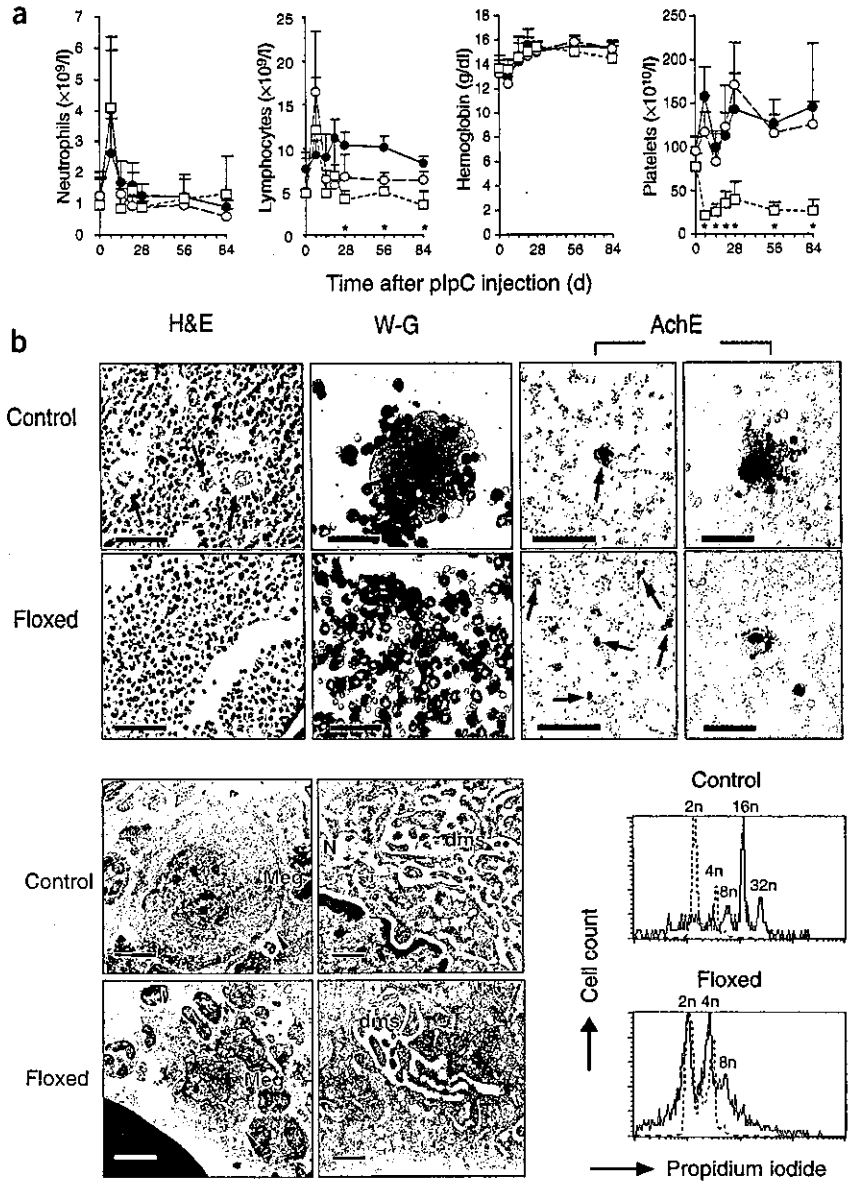

Figure 2 Thrombocytopenia and megakaryocytic maturation arrest of induced AML-1 knockout mice. (**a**) Peripheral blood cell counts of *Runx1*$^{+/+}$*Mx-cre* (control; ●), *Runx1*$^{fl/+}$*Mx-cre* (○) and *Runx1*$^{fl/-}$*Mx-cre* (floxed; □) mice injected with pIpC on days 0, 2 and 4. Results are shown as mean + s.d. (error bars) from four to seven mice. *, $P < 0.01$ for floxed compared with control mice (unequal-variance *t*-test). (**b**) Histochemical analyses of bone marrow. W-G, Wright-Giemsa; AchE, acetylcholinesterase. Arrows indicate megakaryocytes. Scale bars, 50-μm (H&E, W-G, and AchE right panel) or 250-μm (AchE left panel). (**c**) Electron micrographs of bone marrow megakaryocytes. Meg/arrowhead, megakaryocytes; dms, demarcation membranes; N, nucleus. Scale bars, 5-μm (left) or 500-nm (right). (**d**) DNA contents of CD41$^+$ bone marrow cells. – – –, CD41$^-$ fractions for 2*n* and 4*n* controls. Typical results from three experiments are shown (4–8 weeks after pIpC injection).

8), compared with 0.424 ± 0.118 for control mice ($n = 4$); $P = 0.93$ by Wilcoxon rank-sum test) or monocytes (test/competitor = 0.443 ± 0.082 for floxed mice ($n = 8$), compared with 0.940 ± 0.440 for control mice ($n = 4$); $P = 0.35$). The floxed cells also repopulated the megakaryocytic progenitors (Lin$^-$CD41$^+$; Fig. 4b). Given the inability of AML-1-deficient cells to reconstitute the T-cell lineage, we investigated thymocyte development in the absence of AML-1 by analyzing double-negative thymocytes of the recipient mice. We observed a significant block in the maturation of floxed T-cell progenitors at the transition from CD44$^+$CD25$^+$ (DN2) to CD44$^-$CD25$^+$ (DN3) (DN3/DN2 ratio of Ly5.1$^-$Ly5.2$^+$ cells = 0.025 ± 0.029 for floxed mice ($n = 5$), compared with 1.87 ± 1.51 for control mice ($n = 4$); $P < 0.05$; Fig. 4c), indicating that immature T-cell precursors had accumulated in the thymus. These findings, along with the observation that the CLP fraction was not affected in the floxed bone marrow, suggest that AML-1 is not necessary for the maintenance of CLPs, but is required in lymphoid precursors committed to T- or B-cell lineages. Consistent with this, a recent report and our experiments using *lck-Cre*-mediated, T-cell-specific AML-1-knockout mice show that the maturation of T-cell progenitors deficient in AML-1 is blocked at the DN3-DN4 transition (ref. 24 and T.A. *et al.*, unpublished data). Because *lck-Cre* expression becomes evident at the DN3 stage or later, the present study unveiled an important role of AML-1 in the DN2-DN3 transition. However, because of the insufficient contribution of the floxed cells to the B220$^+$ bone marrow fraction (test/competitor = 0.011 ± 0.012 ($n = 8$) compared with 0.306 ± 0.295 for control ($n = 4$)), we could not determine which step in B-cell development was affected by the absence of AML-1. The role of AML-1 in B-cell development might be revealed by other approaches, including the analysis of B-cell lineage-specific AML-1-knockout mice. Although lymphocyte development is substantially blocked at early stages in the absence of AML-1, the detection of AML-1-deleted T and B cells in the periphery of *Runx1*$^{fl/-}$*Mx-cre* mice (Fig. 1b) indicates that some lymphoid progenitors may still survive for a prolonged period and differentiate into mature lymphocytes.

Our data show that lack of AML-1 at the adult stage causes hematopoietic progenitor cell expansion, probably through a partial block in myeloid cell differentiation. This finding agrees with the phenotypes of previously reported mouse models of t(8;21)—carrying human leukemia, in which AML-1/ETO fusion protein is implicated in leukemogenesis through dominant-negative suppression of AML-1 function[19–21]. The loss or dominant-negative suppression of AML-1 function is also found in human myelodysplastic syndromes and familial platelet disorder with predisposition to AML[8,9], both of which are thought to be a preleukemic state. Taken as a whole, our observations suggest that the number of hematopoietic progenitor cells is negatively regulated by AML-1, and that the loss of AML-1 function triggers a preleukemic state. However, the myeloid immaturity and immortalization of bone marrow progenitors observed in AML-1/ETO mice could not be recapitulated in our *Runx1*$^{fl/-}$*Mx-cre* mice. Therefore, AML-1/ETO may not only inhibit AML-1 func-

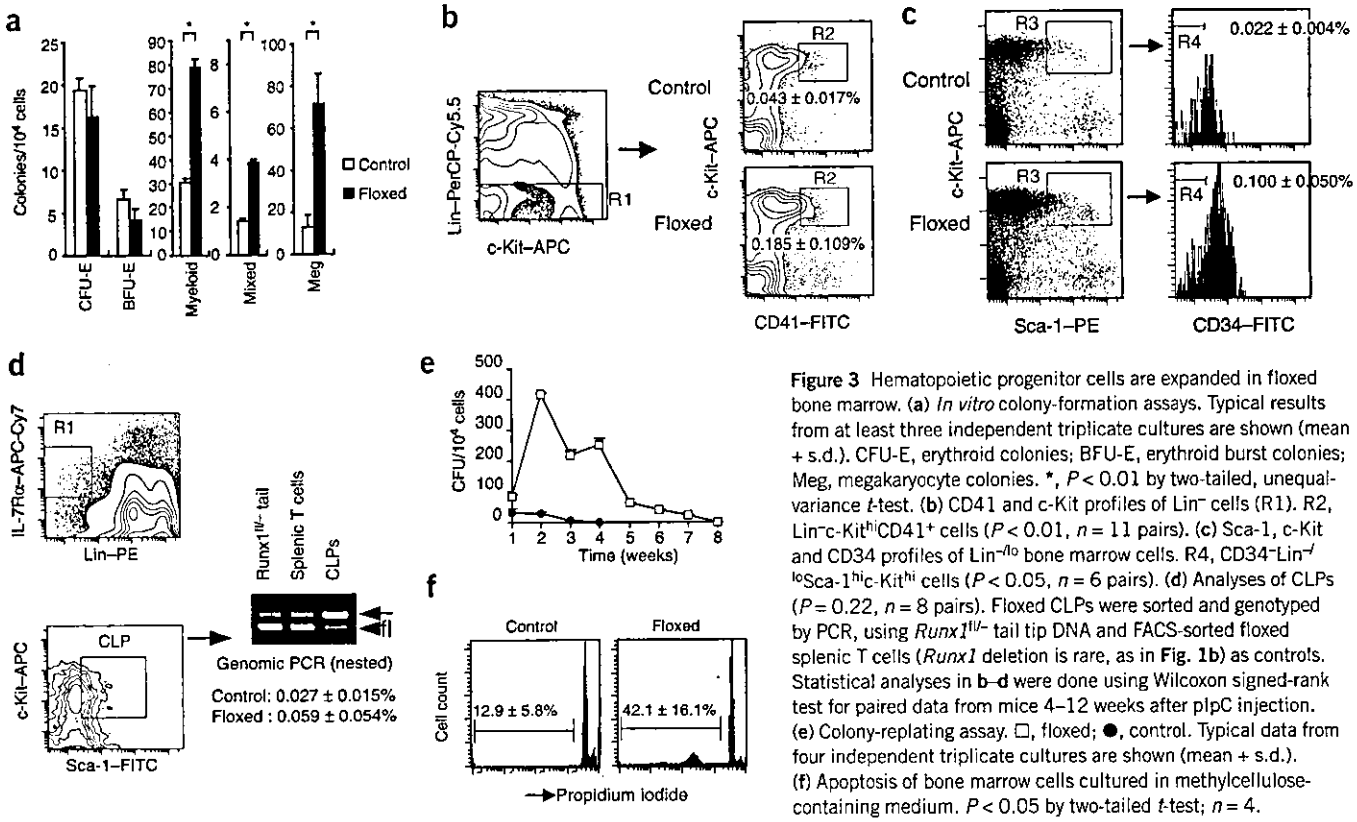

Figure 3 Hematopoietic progenitor cells are expanded in floxed bone marrow. (**a**) *In vitro* colony-formation assays. Typical results from at least three independent triplicate cultures are shown (mean + s.d.). CFU-E, erythroid colonies; BFU-E, erythroid burst colonies; Meg, megakaryocyte colonies. *, $P < 0.01$ by two-tailed, unequal-variance *t*-test. (**b**) CD41 and c-Kit profiles of Lin$^-$ cells (R1). R2, Lin$^-$c-Kit^{hi}CD41$^+$ cells ($P < 0.01$, $n = 11$ pairs). (**c**) Sca-1, c-Kit and CD34 profiles of Lin$^{-/lo}$ bone marrow cells. R4, CD34$^-$Lin$^{-/lo}$Sca-1^{hi}c-Kit^{hi} cells ($P < 0.05$, $n = 6$ pairs). (**d**) Analyses of CLPs ($P = 0.22$, $n = 8$ pairs). Floxed CLPs were sorted and genotyped by PCR, using *Runx1*$^{fl/-}$ tail tip DNA and FACS-sorted floxed splenic T cells (*Runx1* deletion is rare, as in **Fig. 1b**) as controls. Statistical analyses in **b**–**d** were done using Wilcoxon signed-rank test for paired data from mice 4–12 weeks after pIpC injection. (**e**) Colony-replating assay. □, floxed; ●, control. Typical data from four independent triplicate cultures are shown (mean + s.d.). (**f**) Apoptosis of bone marrow cells cultured in methylcellulose-containing medium. $P < 0.05$ by two-tailed *t*-test; $n = 4$.

tion, but may also have the ability to immortalize hematopoietic progenitors.

Although AML-1 is considered to be a master regulator of definitive hematopoiesis, our current study shows that AML-1 is dispensable for prolonged hematopoietic cell engraftment, as well as commitment to the myeloid lineage and at least to double-negative thymocytes in the lymphoid lineage. Our present data also indicate that AML-1 is essential for the terminal differentiation of hematopoietic progenitors of megakaryocytic and lymphocytic lineages, which establishes AML-1 as a regulator with multiple roles in the maintenance of lineage-committed cells in adult hematopoiesis. However, our results also suggest that the maintenance of HSCs and their commitment to more mature progenitors in adult hematopoiesis does not always require a transcription factor essential for hematopoietic ontogeny during embryogenesis, and can be induced by other hematopoietic genes. This is supported by a previous study

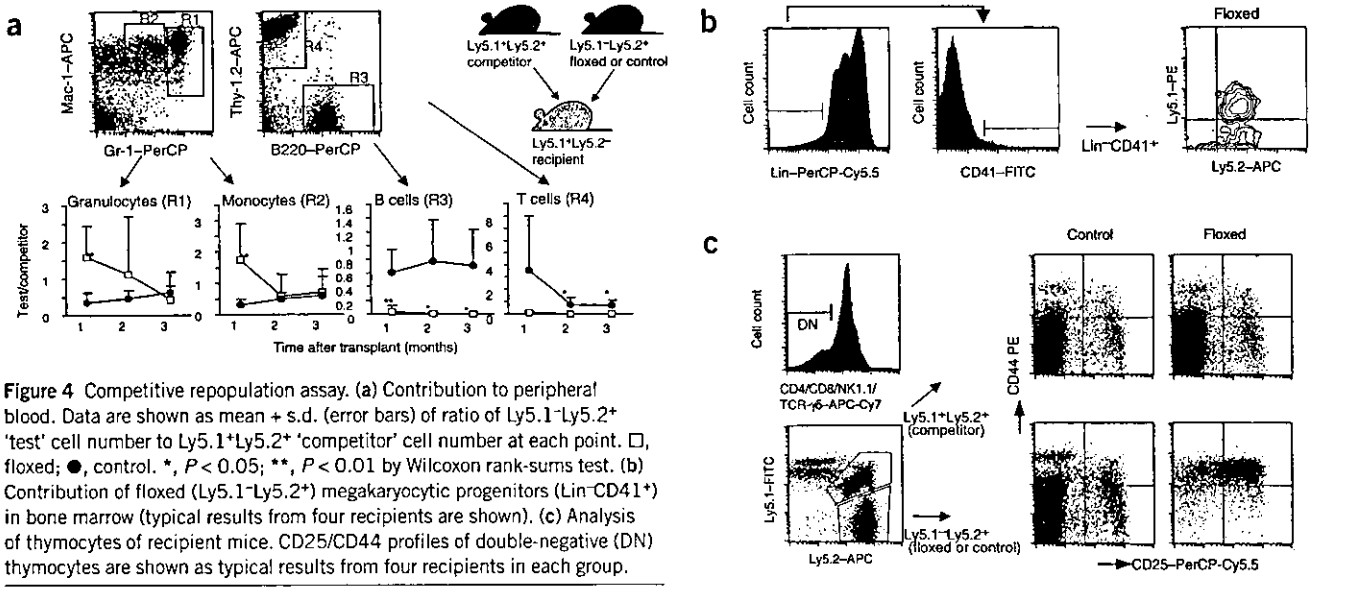

Figure 4 Competitive repopulation assay. (**a**) Contribution to peripheral blood. Data are shown as mean + s.d. (error bars) of ratio of Ly5.1$^-$Ly5.2$^+$ 'test' cell number to Ly5.1$^+$Ly5.2$^+$ 'competitor' cell number at each point. □, floxed; ●, control. *, $P < 0.05$; **, $P < 0.01$ by Wilcoxon rank-sums test. (**b**) Contribution of floxed (Ly5.1$^-$Ly5.2$^+$) megakaryocytic progenitors (Lin$^-$CD41$^+$) in bone marrow (typical results from four recipients are shown). (**c**) Analysis of thymocytes of recipient mice. CD25/CD44 profiles of double-negative (DN) thymocytes are shown as typical results from four recipients in each group.

that showed that SCL/*tal-1*, a transcription factor essential for the development of primitive hematopoiesis during the embryonic stage, is required for the proper differentiation of erythroid and megakaryocytic lineages, but not for the maintenance of HSCs in adult hematopoiesis[25]. To fully understand the intricate process of hematopoiesis, it will be necessary to determine the roles of those hematopoietic genes.

METHODS

Mice. We introduced the targeting vector (Fig. 1a) into TT2 embryonic stem cells[26], and transiently expressed Cre recombinase to generate embryonic stem cell lines carrying the *Runx1*^{fl} or *Runx1*$^{-}$ alleles. Chimeric mice raised by aggregation were crossed to the C57BL/6 background, and were mated to interferon-inducible *Mx-cre* transgenic mice[10]. *Mx-cre* expression was induced by intraperitoneally injecting 250 μg of pIpC, on three alternate days, into 4- to 8-week-old mice[10]. C57BL/6-Ly5.1 congenic and C57BL/6-Ly5.1/Ly5.2 F_1 mice were used for competitive repopulation assays. Mice were kept at the Animal Center for Biomedical Research, University of Tokyo, according to institutional guidelines.

Genotyping. For PCR genotyping, cells were lysed in a lysis buffer (0.3% Tween 20, 0.3% NP-40, and 120 μg/ml proteinase K in 1× TE buffer) at 55 °C for 1 h, followed by inactivation at 80 °C for 10 min. DNA was amplified using primers f2 (5′-ACAAAACCTAGGTGTACCAGGAGAACAAGT-3′), f120 (5′-CCCTGAAGACAGGAGAAGTTTCCA-3′) and r1 (5′-GTCTACTC-CTTGCCTCAGAAAACAAAAAC-3′) for the first PCR reaction, and nested primers f1 (5′-AAAACCTAGGTGTACCAGGAGAACAAGTC-3′), f101 (5′-TTCCAGGTCAACTCTCTCACCTCTC-3′) and r5 (5′-ATCTGAGTTGGCC TAATTTCCCTTTG-3′) for the second reaction, to detect the 280-base pair *Runx1*$^{-}$ and 220-base pair *Runx1*^{fl} products. Southern blot analyses of DNA samples digested with *Eco*RI were done according to standard protocols, using a 5′ *Eco*RI-*Bgl*II genomic probe (Fig. 1a).

Analyses of blood cells. Peripheral blood was counted using an automated hemacytometer, and leukocytes were morphologically classified to calculate neutrophil and lymphocyte counts. Mice were analyzed for bone marrow morphology 2 months after pIpC administration. For histological examination, sectioned femoral bone marrow specimens were stained with H&E, and cytocentrifuged specimens were stained with Wright-Giemsa or for acetylcholinesterase as previously described[11]. Peritoneal exudative cells were collected by washing the peritoneal cavities of mice 4 h after intraperitoneal injection of 2 ml of 2% casein in PBS. Splenocytes were labeled with antibodies to Thy-1.2 (for T cells) or B220 (for B cells), conjugated to magnetic microbeads to collect splenic lymphocytes using a MACS LS+ system (Miltenyi Biotec). The cells were checked for purity by flow cytometry (>97%; data not shown).

Ultrastructural studies. Femoral bone marrow samples prepared 4 weeks after pIpC injection as previously described[27] were examined with a JEOL 1200CX electron microscope.

Flow cytometry and cell sorting. All monoclonal antibodies and fluorochromes were purchased from BD PharMingen. To measure bone marrow progenitor cells other than CLPs, cells were stained with FITC-conjugated antibodies to CD41 or CD34, phycoerythrin (PE)-conjugated antibody to Sca-1, allophycocyanin (APC)-conjugated antibody to c-Kit, and biotin-conjugated antibodies to lineage (Lin) markers (CD3ε, CD4, CD8a, B220, Gr-1, Mac-1 and Ter119), and visualized with streptavidin-PerCP-Cy5.5. For CLP cell fractions, cells were stained with Lin-PE, Sca-1-FITC, c-Kit-APC and IL-7Rα–biotin/streptavidin-APC-Cy7. Stained samples were analyzed using either FACSCalibur or BD LSRII (BD Biosciences). For sorting CLP cells, Lin^{+} were predepleted from bone marrow cells using the MACS LD system (Miltenyi Biotec). The remaining fraction was stained for CLP as described above and sorted using a FACSVantage cell sorter. The cell sorter was calibrated to achieve >98% purity for Thy-1.2^{+} cells stained with Thy-1.2–APC. Approximately 1,000 CLP cells were genotyped by PCR. To analyze competitively repopulated cells, cells were stained with Ly5.2–FITC, Ly5.1–PE, Gr-1–biotin/streptavidin–PerCP and Mac-1–APC for myeloid cells, and with Ly5.2–FITC, Ly-5.1–PE, B220–PerCP and Thy-1.2–APC for T and B lymphocytes. Thymocytes were stained with Ly5.1–FITC, Ly5.2–APC, CD25– PerCP-Cy5.5, CD44–PE and biotin-conjugated antibodies to CD4, CD8, NK1.1 and TCR-γδ, and visualized by streptavidin–APC-Cy7 for analyzing double-negative thymocytes. Bone marrow megakaryocytic progenitors were stained with CD41–FITC, Ly-5.1–PE, Ly-5.2–APC and Lin–biotin/streptavidin-PerCP-Cy5.5. Two-color flow cytometric analysis of the DNA content of bone marrow megakaryocytes stained with CD41–FITC was performed as previously described[28].

***In vitro* hematopoietic colony-forming assays.** For CFU-Meg, 2.5×10^4 bone marrow cells from mice 4–8 weeks after pIpC injection were cultured in 1 ml of α-MEM containing 0.8% methylcellulose, 1% BSA, 30% FBS, 100 μM 2-mercaptoethanol and 10 units of mouse thrombopoietin. For other (myeloid and erythroid) colonies, 5×10^4 cells were cultured in 1-ml of IMDM containing 0.8% methylcellulose, 1% BSA, 30% FBS, 100-μM 2-mercaptoethanol, 100-ng/ml of mouse stem cell factor, 5-ng/ml of mouse interleukin-3 and 7.5 units/ml of human erythropoietin (all growth factors were generously provided by Kirin Brewery). Colonies were counted after 3 d (for erythroid colonies), 5 d (for erythroid bursts and myeloid colonies), 7 d (for mixed colonies) or 8 d (for CFU-Meg) of culture in 5% CO_2 at 37 °C. For replating experiments, the whole myeloid and erythroid culture was pooled on day 7 and washed twice, and 1×10^4 cells were subjected to subsequent culture in the same medium. Scoring for colonies and reculturing were repeated every 7 d.

Detection of apoptotic cells. Whole myeloid and erythroid methylcellulose cultures were pooled on day 7 of culture, washed, fixed and stained with propidium iodide for analysis by flow cytometry to detect apoptotic cells (DNA content < 2*n*) as previously described[29].

Competitive repopulation assay. X-ray-irradiated (9.5-Gy, 0.3-Gy/min, unfractionated) recipient mice were intravenously injected with a mixture of 1×10^5 each of unfractionated bone marrow cells from 'test' mice (floxed or control mice, 8–12 weeks after pIpC injection) and competitor mice. Peripheral blood was analyzed monthly, and bone marrow cells and thymocytes were analyzed 3 months after transplantation by flow cytometry.

ACKNOWLEDGMENTS

We thank S. Aizawa for providing us with TT2 ES cells; T. Komori for *Runx1* genomic fragments; J. Takeda for *Mx-cre*-transgenic mice; and thank K. Kumano, A. Kunisato and other members of H.H.'s lab for critical discussion. This work was supported in part by a Grant-in-Aid for Scientific Research (KAKENHI 13307029, 15689015) from the Japan Society for the Promotion of Science, and by Health and Labour Sciences Research grants from the Ministry of Health, Labour and Welfare.

COMPETING INTERESTS STATEMENT

The authors declare that they have no competing financial interests.

Received 4 November 2003; accepted 20 January 2004
Published online at http://www.nature.com/naturemedicine/

1. Okuda, T., van Deursen, J., Hiebert, S.W., Grosveld, G. & Downing, J.R. AML1, the target of multiple chromosomal translocations in human leukemia, is essential for normal fetal liver hematopoiesis. *Cell* **84**, 321–330 (1996).
2. Wang, Q. *et al.* Disruption of the *Cbfa2* gene causes necrosis and hemorrhaging in the central nervous system and blocks definitive hematopoiesis. *Proc. Natl. Acad. Sci. USA* **93**, 3444–3449 (1996).
3. Mukouyama, Y. *et al.* The AML1 transcription factor functions to develop and maintain hematogenic precursor cells in the embryonic aorta-gonad-mesonephros region. *Dev. Biol.* **220**, 27–36 (2000).
4. Yokomizo, T. *et al.* Requirement of Runx1/AML1/PEBP2αB for the generation of haematopoietic cells from endothelial cells. *Genes Cells* **6**, 13–23 (2001).
5. North, T.E. *et al.* Runx1 expression marks long-term repopulating hematopoietic stem cells in the midgestation mouse embryo. *Immunity* **16**, 661–672 (2002).
6. Tenen, D.G., Hromas, R., Licht, J.D. & Zhang, D.E. Transcription factors, normal myeloid development, and leukemia. *Blood* **90**, 489–519 (1997).
7. Lutterbach, B. & Hiebert, S.W. Role of the transcription factor AML-1 in acute leukemia and hematopoietic differentiation. *Gene* **245**, 223–235 (2000).
8. Imai, Y. *et al.* Mutations of the AML1 gene in myelodysplastic syndrome and their functional implications in leukemogenesis. *Blood* **96**, 3154–3160 (2000).
9. Song, W.J. *et al.* Haploinsufficiency of CBFA2 causes familial thrombocytopenia with pro-

pensity to develop acute myelogenous leukaemia. *Nat. Genet.* **23**, 166–175 (1999).
10. Kuhn, R., Schwenk, F., Aguet, M. & Rajewsky, K. Inducible gene targeting in mice. *Science* **269**, 1427–1429 (1995).
11. Jackson, C.W. Cholinesterase as a possible marker for early cells of the megakaryocytic series. *Blood* **42**, 413–421 (1973).
12. Kaushansky, K. The enigmatic megakaryocyte gradually reveals its secrets. *Bioessays* **21**, 353–360 (1999).
13. Elagib, K.E. *et al.* RUNX1 and GATA-1 coexpression and cooperation in megakaryocytic differentiation. *Blood* **101**, 4333–4341 (2003).
14. Shivdasani, R.A., Fujiwara, Y., McDevitt, M.A. & Orkin, S.H. A lineage-selective knockout establishes the critical role of transcription factor GATA-1 in megakaryocyte growth and platelet development. *EMBO J.* **16**, 3965–3973 (1997).
15. Takahashi, S. *et al.* Role of GATA-1 in proliferation and differentiation of definitive erythroid and megakaryocytic cells *in vivo*. *Blood* **92**, 434–442 (1998).
16. Hodohara, K., Fujii, N., Yamamoto, N. & Kaushansky, K. Stromal cell-derived factor-1 (SDF-1) acts together with thrombopoietin to enhance the development of megakaryocytic progenitor cells (CFU-MK). *Blood* **95**, 769–775 (2000).
17. Osawa, M., Hanada, K., Hamada, H. & Nakauchi, H. Long-term lymphohematopoietic reconstitution by a single CD34-low/negative hematopoietic stem cell. *Science* **273**, 242–245 (1996).
18. Kondo, M., Weissman, I.L. & Akashi, K. Identification of clonogenic common lymphoid progenitors in mouse bone marrow. *Cell* **91**, 661–672 (1997).
19. Rhoades, K.L. *et al.* Analysis of the role of AML1-ETO in leukemogenesis, using an inducible transgenic mouse model. *Blood* **96**, 2108–2115 (2000).
20. Higuchi, M. *et al.* Expression of a conditional AML1-ETO oncogene bypasses embryonic lethality and establishes a murine model of human t(8;21) acute myeloid leukemia. *Cancer Cell* **1**, 63–74 (2002).
21. de Guzman, C.G. *et al.* Hematopoietic stem cell expansion and distinct myeloid developmental abnormalities in a murine model of the AML1-ETO translocation. *Mol. Cell. Biol.* **22**, 5506–5517 (2002).
22. Szilvassy, S.J., Humphries, R.K., Lansdorp, P.M., Eaves, A.C. & Eaves, C.J. Quantitative assay for totipotent reconstituting hematopoietic stem cells by a competitive repopulation strategy. *Proc. Natl. Acad. Sci. USA* **87**, 8736–8740 (1990).
23. Lagasse, E. & Weissman, I.L. Flow cytometric identification of murine neutrophils and monocytes. *J. Immunol. Methods* **197**, 139–150 (1996).
24. Taniuchi, I. *et al.* Differential requirements for Runx proteins in CD4 repression and epigenetic silencing during T lymphocyte development. *Cell* **111**, 621–633 (2002).
25. Mikkola, H.K. *et al.* Haematopoietic stem cells retain long-term repopulating activity and multipotency in the absence of stem-cell leukaemia SCL/tal-1 gene. *Nature* **421**, 547–551 (2003).
26. Yagi, T. *et al.* A novel ES cell line, TT2, with high germline-differentiating potency. *Anal. Biochem.* **214**, 70–76 (1993).
27. Breton-Gorius, J., Reyes, F., Duhamel, G., Najman, A. & Gorin, N.C. Megakaryoblastic acute leukemia: identification by the ultrastructural demonstration of platelet peroxidase. *Blood* **51**, 45–60 (1978).
28. Jackson, C.W., Brown, L.K., Somerville, B.C., Lyles, S.A. & Look, A.T. Two-color flow cytometric measurement of DNA distributions of rat megakaryocytes in unfixed, unfractionated marrow cell suspensions. *Blood* **63**, 768–778 (1984).
29. Sherwood, S.W. & Schimke, R.T. Cell cycle analysis of apoptosis using flow cytometry. *Methods Cell Biol.* **46**, 77–97 (1995).